Debris Flows: Recent Advances in Experiments and Modeling

Diego Berzi[a], James T. Jenkins[b], Michele Larcher[c]

[a] Department of Environmental, Hydraulic, Infrastructures and Surveying Engineering, Politecnico di Milano, Milan, Italy
[b] School of Civil and Environmental Engineering, Cornell University, Ithaca, NY, USA
[c] Department of Civil and Environmental Engineering, Trento University, Trento, Italy

1. Introduction

A debris flow is a mixture of water and particles driven down a slope by gravity. They typically consist of unsteady, non-uniform surges of mixtures of muddy water and high concentrations of rock fragments of different shapes and sizes. In its traverse down a slope, a debris flow may accumulate large amounts of material and transport it with high velocities. Because of modifications in rainfall patterns, the urbanization of mountain environments, and the abandonment of cultivated land in recent decades, the frequency of debris flows and the hazards associated with them have dramatically increased and they pose a significant threat to life and property (e.g., McPhee 1989).

While we are aware that natural debris flows typically consist of unsteady, non-uniform surges of heterogeneous mixtures, exhibit strong grain-size segregation, and may involve distributions of fluid pressure that are not hydrostatic (Iverson, 1997), our intent here is to emphasize steady flows of idealized composition. These flows may be uniform or non-uniform and consist of water and identical particles or water and a mixture of particles with two diameters. Our interest is in the physics appropriate to their description. We focus on what we believe are the essential features of most, if not all, debris flows; these are the collisions between particles, mitigated by the interstitial fluid (e.g., Courrech du Pont, et al. 2003), that provide the mechanism for momentum transfer within the particle phase, and the particle-fluid interactions that provide forces to the particle phase associated with buoyancy, fluid drag, and fluid pressure.

Flows over either rigid or previously deposited erodible beds are possible; the latter incorporate particles into the flow until a steady, uniform balance of forces is attained within the flow. The flows that result may involve depths of water greater than or less than the depth of the flowing particles. The former we refer to as over-saturated, the latter as under-saturated. All or part of the region of dry particles in an under-saturated flow may be sheared. The existence of under-saturated and over-saturated flows reinforces the need to distinguish between the two phases and, in particular, between their depths.

The experiments of Armanini, et al. (2005) indicate that there is a collisional exchange of particle momentum through the particle phase that decreases near an erodible bed. This may be due to the development of longer lasting particle interactions and/or an increased influence of the

fluid on the inter-particle interactions as the bed is approached. Also, the location of the erodible bed is seen to fluctuate in both space and time. This emphasizes the need for a better understanding of the physics that defines the interface between the continuous shearing flow above it and the intermittent creeping flow below (Komatsu, et al. 2001).

Early models of debris flows treated the mixture as a single homogeneous material and employed a non-Newtonian rheology to incorporate the effect of the particle interactions (e.g., Johnson 1984, Takahashi 1991, Coussot 1994, Chen 1998, Brufau, 2000). The rheologies adopted range from visco-plastic, with yield followed by linearly viscous shear stress, to collisional, with shear and normal stresses quadratic in the shear rate (Bagnold, 1954). However, as emphasized by Iverson (2003), such single-phase models cannot capture the interactions between the fluid and particle phases that are crucial to the description of the observed behaviour of debris flows. He emphasizes that the nature of small scale interactions between and among the particles and fluid differ greatly with time and position within the debris flow and focuses on the influence that local pore fluid pressure can have on the mobility of the particle phase.

Iverson (1997) and others (e.g., Pittman and Le, 2005) go beyond the single-phase model for the mixture by incorporating the pore pressure and, more recently (Iverson, 2009), particle concentration as additional fields that characterizes the local state of the material. The rheology of the particle phase is described using a rate-independent plasticity that distinguishes between compression and extension. These models are typically used in depth-averaged equations. However, such models do not distinguish between the depths of the particle and fluid phases; and, as a consequence, they must employ changes in concentration to describe pore pressure changes and attribute the formation of snouts and lateral levees to size segregation in the particle phase. In this article, we attempt to establish that the appropriate particle rheology in a two-phase formulation is likely to include a rate-dependent component and that it is necessary to distinguish between the depths of the two phases. In doing so, a description of the formation of snouts and lateral levees is obtained that is associated with the difference in depths and rheology of the fluid and particle phases, independent of any size segregation of particles.

We first describe recent laboratory experiments on steady, inclined flows of mixtures of water and a single idealized granular phase that focus on the differences in the depths and the velocity of the two phases and that provide evidence for the importance of collisional exchange of momentum and energy between the particles. We then indicate how a relatively simple rate-dependent rheological model for the particles that incorporates yield may be used in the context of a two-phase mixture theory that distinguishes between the depths of the fluid and particle phases to reproduce what is seen in the experiments on both uniform and non-uniform flows. Finally, because a phenomenological extension of kinetic theory for a dense inclined flows of identical particles has recently been developed (e.g. Jenkins and Berzi 2010), we outline a kinetic theory for dense, inclined flows of two types of particles and water as a possible though untested alternative to existing phenomenological theories (e.g. Gray 2010). The result is not meant to be

an exhaustive review of the experiments on and the modelling of debris flow, but a report of recent advances.

2. Experiments

As already mentioned, debris flows are complicated phenomena that involve mixtures of air, water, sediments with wide grain size distributions and, sometimes, vegetal material, driven by gravity down slopes. The interactions between the different phases are still not completely clear, making it difficult for scientists and engineers to predict the triggering, the propagation, and the arrest of these flows.

Even excluding the role of the vegetal material, the presence of large solid fractions and wide particle size distributions results in a very complicated interaction between the solids and the interstitial fluid. In fact, the finer fraction of the granular phase, e.g. clay and silt, can mix almost perfectly with the water and form a homogeneous, very viscous, and possibly non-Newtonian interstitial fluid, in which the liquid and the solid constituents can no longer be distinguished (e.g., Armanini *et al.* 2003). In contrast, each grain belonging to the larger solid fractions has an instantaneous velocity that typically differs from those of the surrounding fluid and the neighbouring particles (e.g. Tubino and Lanzoni 1993). This is an indication that a two-phase approach should be adopted in the physical and mathematical modelling. Moreover, even if the finer particles that are mixed with the water are excluded, non-uniform distributions of particle concentration and sizes are observed throughout the flow depth.

Given the complex picture described above, researchers have simplified the framework of their analysis as much as possible without eliminating the essential features of real debris flows. *Ad hoc* experiments have been performed in order to study the behaviour of debris flow and derive proper rheological relations to be used in mathematical models suitable for risk mapping, the formulation of design criteria for control works aimed at hazard mitigation, and the development of warning systems.

In this section, we will present a synthesis of published experiments on steady uniform and non-uniform flows of mixtures of water and idealized particles. We will not present any result for dry granular flows; because, in our view, the role of the water is fundamental to the generation and propagation of a debris flow. Nor will we present any experiments in which debris flows are treated as a single phase. For simplicity, we will also exclude from this article the influence of woody debris, and we will focus solely on the propagation problem, setting aside the treatment of initiation and arrest.

2.1 Steady, uniform flow

Although debris flow are natural phenomena that endanger lives and property in many regions of the world, the first organized scientific analysis of their nature, occurrence, development, and deposition is relatively recent (Takahashi 1977, 1978, 1980, 1981, 1991). Takahashi documented and analysed numerous debris flows and adapted geotechnical approaches and granular flow theories (Bagnold 1954) to study their mechanics. Until then, almost all of the available experimental work was devoted to dry granular flows or to non-Newtonian single-phase fluids. Takahashi was the first and, until now, among the few researchers that carried out laboratory experiments on debris model flows that consisted of mixtures of water and sediments at high concentration. Later experiments on liquid-granular mixtures devoted to the understanding of debris flow mechanics are due to Tubino and Lanzoni (1993) and Armanini *et al.* (2005). To our knowledge, the latter experiments are the only ones in which the particle and the fluid volume fluxes were separately measured.

Takahashi (1991) described the typical propagation of debris flows in terms of surges, each characterized by a steep front, a central body, and a tail. While the analysis of the front is important for evaluating the impact forces on possible countermeasures and buildings, the propagation of many debris flows is governed by the mechanics relevant to the body, in which the flow can often be assumed to be uniform. Indeed, in most cases, the depth of the body remains almost constant during propagation, while its length increases because of the entrainment of material (Takahashi 1991, Davies 1988, 1990). Consequently, the experimental study of steady, uniform, highly concentrated granular-fluid mixtures in laboratory flumes is directly relevant to the understanding of debris flows.

Tubino and Lanzoni (1993) made careful experimental observations of flow depth, time-averaged velocity, velocity fluctuations, and bulk concentration in inclined, steady, uniform debris flows in an open channel. Their aim was to employ their experimental results to build a model for the overall rheology of a debris flow in the grain-inertia regime defined by Bagnold (1954), in which the momentum exchange is dominated by inter-particle collisions. This regime is equivalent to what Takahashi (1991) called a stony debris flow. Most of the experiments of Tubino and Lanzoni (1993) are on steady, uniform flows. In these, they show that the shape of the grains and the type of boundaries play an important role on the nature of the flow. For the experiments, they used a 10 m long and 20 cm wide channel, with a slope adjustable up to 31° and transparent sidewalls. In each experiment, a 9 to 10 cm thick layer of grains was placed on the base of the flume before it was saturated with water. A permeable ground sill was installed at the downstream end of the flume in order to prevent loss of the bed. A tank was positioned at the head of the flume and was filled with water. The release of a known volume flux of water from the tank and the consequent bed erosion led to the formation of a debris flow that propagated downstream for about 20 seconds without producing a significant erosion of the bed in the downstream part of the flume. The thickness of the saturated bed of particles affected the duration of the experiment, but had no influence on the flow characteristics. The volume flux of

water and the initial slope of the flume were the only input parameters, while the solid concentration resulted from the entrainment of grains in the upper part of the flume.

The measurements of the time-averaged and fluctuating velocity were performed analysing videos recorded through the flume sidewall at a frequency of 50 frames per second. However, this is a very low frequency for the measurement of velocity fluctuations; Armanini *et al.* (2005) and Larcher *et al.* (2007) indicate that frame-rates above 250 frames per second should be employed in order to extract statistically significant profiles of the velocity fluctuations. Tubino and Lanzoni (1993) also traced particle trajectories to study particle interactions and the mechanisms responsible for stress generation. Particles were observed to move along quasi-rectilinear trajectories, because secondary flows were inhibited by the large concentration. In addition, videos recorded from above the flume did not show significant non-uniformity in the flow velocity across the channel, providing some validation for the hypothesis that the wall measurements were representative of what happened within the flow. They performed experiments using glass spheres and two types of gravel, whose characteristics are summarized in Table 3.

For a given volume flux of water, the authors observed three possible flow behaviours, depending on the initial bed slope. For mild slopes, less than 14° for gravel and 9° for glass beads, the amount of sediments entrained from the erodible bed was not sufficient to develop a fully saturated flow and over-saturated debris flows were generated, with a clear water layer on top. For moderate slopes, in the range 14° to 20°, for gravel, and 9° to 12°, for the glass beads, fully saturated debris flows were observed. At larger slopes, uniform flows could not be observed, because the entrainment of grains from the bed determined a progressively increasing depth of the debris flow. The time-averaged velocity profiles observed at the wall are similar to those of Armanini et al. (2005) and will be discussed with them in the following. The experimental measurements of particle and fluid volume fluxes and bed slope are given in Section 3.

Armanini et al. (2005) investigated steady, uniform flows of water and plastic cylinders in a rectangular inclined flume. They developed a recirculating system that consisted of a glass-walled flume, 20 cm wide and 6 m long and a conveyor system equipped with a flexible belt that could be driven at a speed up to 5 m/s. The mixture of water and plastic cylinders, characterized by an equivalent spherical diameter of 3.7 mm and a density of 1540 kg/m^3, is collected in a hopper at the flume outlet and delivered to the top of the flume by the conveyor system. The flume and the conveyor system can be tilted independently and permit steady flows of liquid-granular mixtures at slopes up to 25°, with no upper limit on the solid fraction. In their experiments, the variables controlled were the total volume of particles and water (the mixture volume) and the slope of the channel.

Once the mixture volume and the slope of the flume were fixed, flows of the mixture were established over a rigid, non-erodible base or over an erodible bed. Flows over an erodible bed

were possible only for a sufficiently large mixture volume and, at least for the plastic particles described above, for slopes up to about 13°. When the flume was filled with smaller volumes of the mixture, both kinds of steady, uniform flow could be observed within a single experimental run, with a sharp transition between the two (Fig. 1). The transition between the rigid and erodible bed migrated in the upstream and downstream directions when the mixture volume was, respectively, increased and decreased. Above an inclination of 13° only flows over a rigid bed were observed.

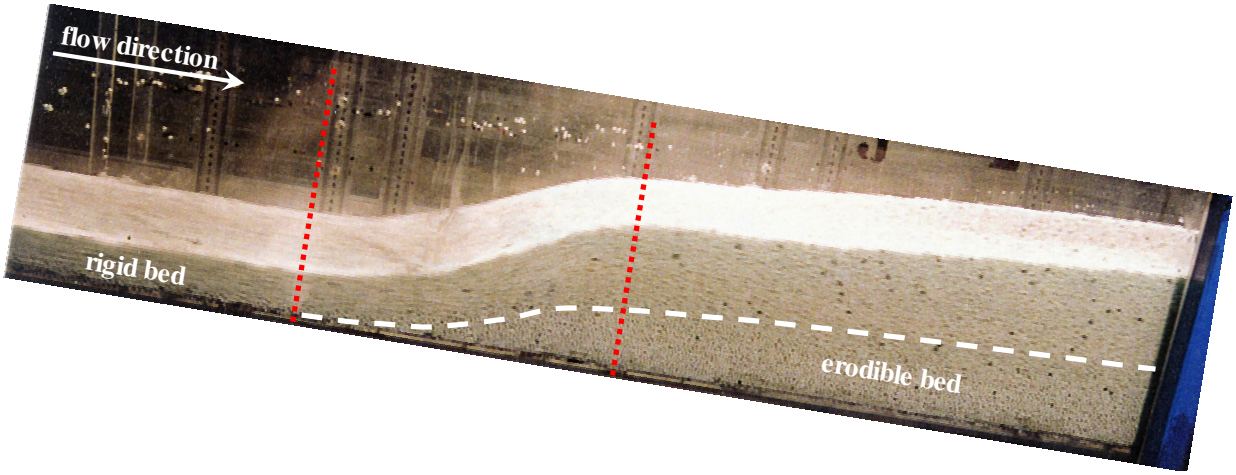

Fig. 1. Example of flows over a rigid and over an erodible bed observed within a single experimental run. The white dashed line represents the limit between moving particles and particles at rest. The transition between the two types of flows is observed in a very limited region (Fraccarollo *et al.* 2007).

For steady, uniform flows over an erodible bed, the authors distinguished three cases, consistent with the definition of Takahashi (1991), depending on whether the height of the flowing particles was equal to the height of the flowing water (a saturated debris flow), the height of the flowing particles was less than the height of the flowing water (an over-saturated debris flow) or the height of the flowing particles was greater than the height of the flowing water (an under-saturated debris flow). As already mentioned, the latter condition was not observed by Tubino and Lanzoni (1993). Multiple exposure views of the flow as seen through the transparent sidewall obtained from a segment of five consecutive frames for each of the three cases described above, and for the case of flow over a rigid bed, are shown in Fig. 2.

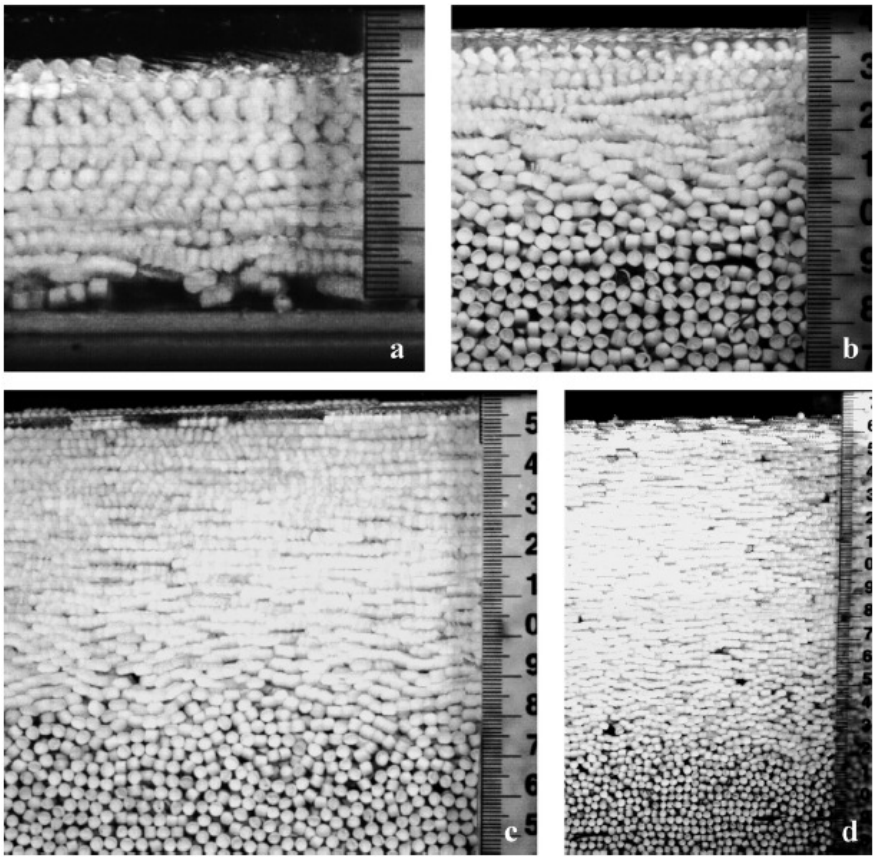

Fig. 2. Multiple exposure views of the flow as seen through the transparent sidewall of the flume (Larcher *et al.* 2007): (a) flow over a rigid bed; (b) over-saturated, (c) saturated and (d) under-saturated flows over an erodible bed.

In steady, uniform flows over a rigid bed, the slope of the flow is equal to the slope of the flume and the concentration is determined solely by the volumes of sediments and water present in the flume-belt system. In contrast, for flows over an erodible bed, the common slope of the bed and the free surface of the flow. It was found to differ from that of the flume and to depend on the ratio between the particle and the total volume flux (Fig. 3). This is one of the main results of their work. These experiments also showed that the ratio of the heights of the water and particles (later referred to as degree of saturation) increased as the slope was decreased (Fig, 4) and that fully-saturated debris flows took place only in a very limited range of bed slopes around 8°.

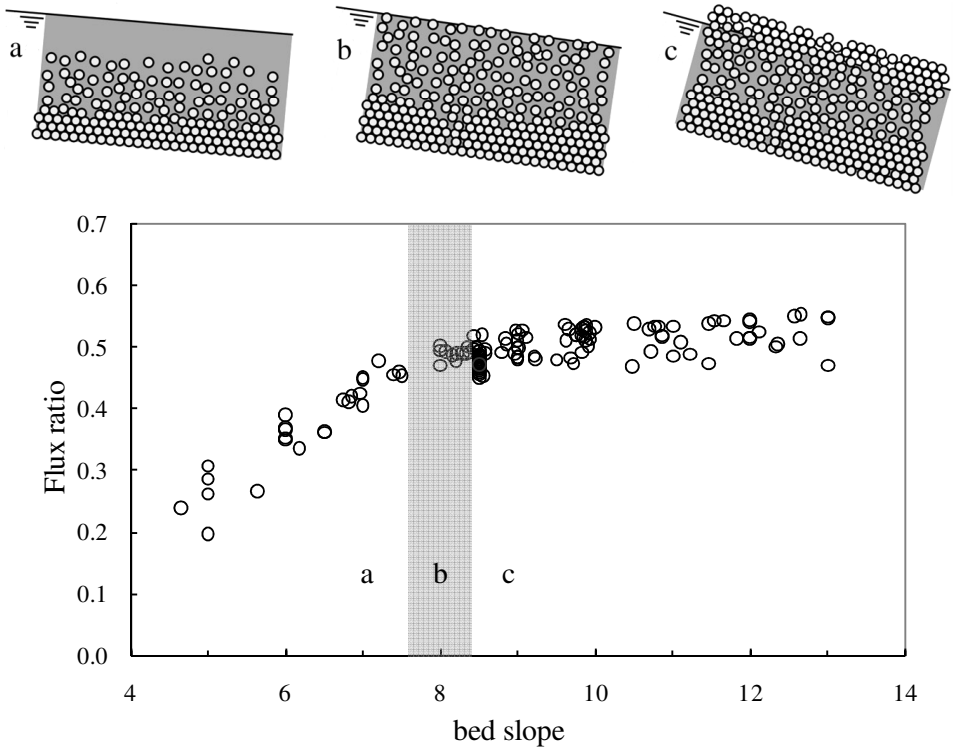

Fig. 3. Experimental relationship between the ratio of particle flux to total flux and the bed slope for experiments over an erodible bed (Larcher *et al.* 2007, Fraccarollo *et al.* 2007). Saturated flows are observed in the bed slope range identified by the gray band (b), over-saturated flows for milder slopes (a) and under-saturated flows for steeper slopes (c).

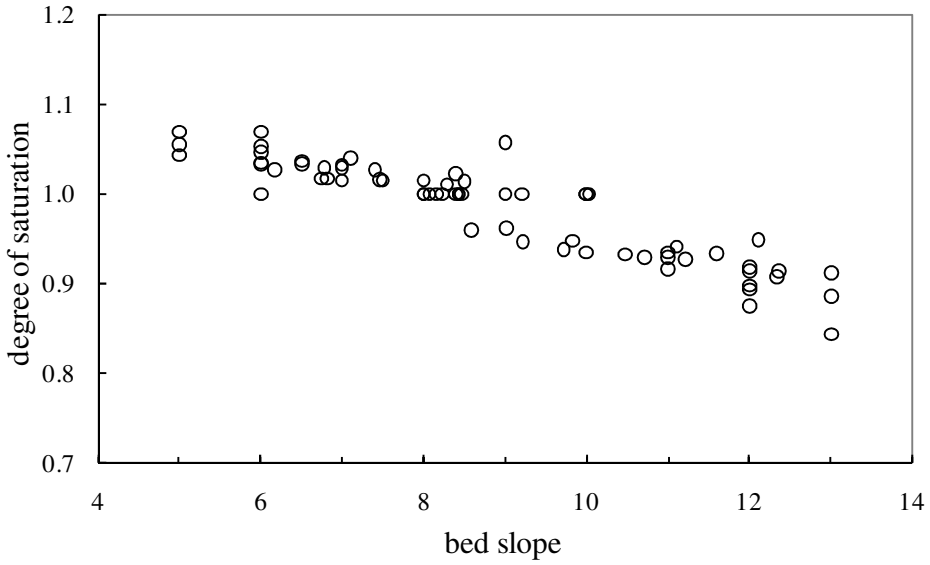

Fig. 4. Experimental measurements of the degree of saturation as a function of the bed slope for the flows over erodible beds (Fraccarollo *et al.* 2007).

Using high-speed video imaging through the flume sidewall and robust imaging analysis (Capart *et al.* 2002, Spinewine *et al.* 2003, Spinewine *et al.* 2010), Armanini et al. (2005) were able to measure the distribution of average particle velocity, concentration, and the strength of the particle velocity fluctuations (granular temperature) through the depth of the flow (Fig. 5) and to make comparisons with the predictions of the collisional theories. For details of the measurements, the reader is referred to Larcher *et al.* (2007), where information can be found on how to access the complete dataset.

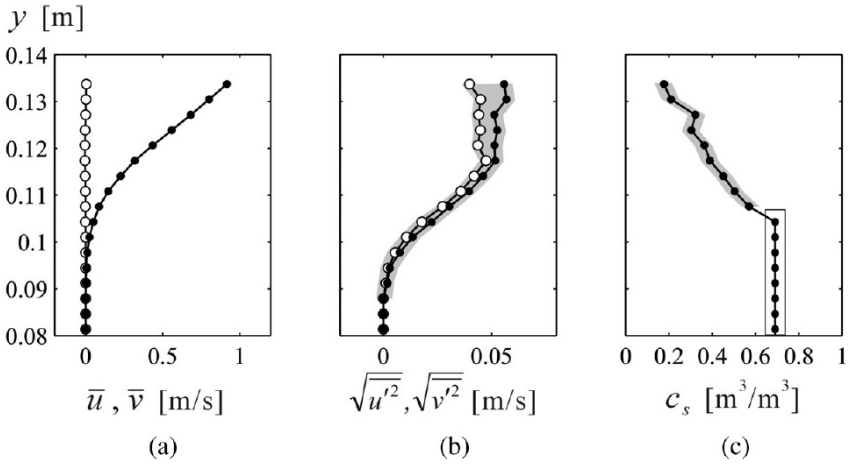

Fig. 5. Profiles normal to the bed for a typical saturated flow over an erodible bed (Larcher *et al.* 2007): (a) longitudinal (dots) and normal (circles) mean velocity; (b) longitudinal (dots) and normal (circles) root-mean-squared fluctuation velocity; (c) concentration. The gray bands represent error bounds, while in panel (c) the frame box surrounds points in the quasi-static bed at which the concentration estimator exceeded the maximum possible volume fraction.

The experiments showed a stratification of rheological regimes inside the flow domain, with some parts dominated by collisional interactions and other parts characterized by large concentrations and more order. In the latter parts, particles interacted through sustained contacts, often moving in organized chains parallel to the bed. Chains of particles were observed, in particular, near the surface of erodible beds. The authors showed that the Bagnold (1954) theory and classic kinetic theory (Jenkins and Hanes 1998) were appropriate tools for the description of the flow in the less dense, collisional layers, while they failed to describe the flow features in the dense layers. They also showed that the local Stokes number - the ratio of the particle inertia to the viscous force exerted on it - had a strong variability throughout the flow depth, and that the transition region between the regimes of collisional and enduring contact was associated with Stokes numbers in the range 5 to 10. In the transition region, Armanini *et al.* (2009) later observed intermittency between the two regimes.

Finally, it is worth noting that mean velocity and granular temperature profiles similar to those reported by Armanini et al. (2005) for the over-saturated case have been experimentally observed in the case of classic sediment transport (Fraccarollo and Rosatti 2010), suggesting that the analysis of debris flows may be extended to deal with more common hydraulic phenomena.

2.2 Steady, non-uniform flow

Although we have already underlined the importance of investigating steady, uniform flows, in order to understand particle-particle and fluid-particle interactions, natural debris flows are often unsteady and inevitably exhibit non-uniform features. Consequently, it natural to consider next laboratory experiments that on these more complex flows. In particular, Davies (1988, 1990) investigated, at laboratory scale, a steady, non-uniform debris flow. He overcame any problem associated with the finite length of the flume by employing a moving-bed apparatus (Fig. 6). In this, a non-uniform wave remains stationary, while the bed moves upwards at constant velocity. The channel walls are fixed, while the bed velocity can be adjusted in order that the grains and the interstitial fluid remain stationary, on average, with respect to the walls.

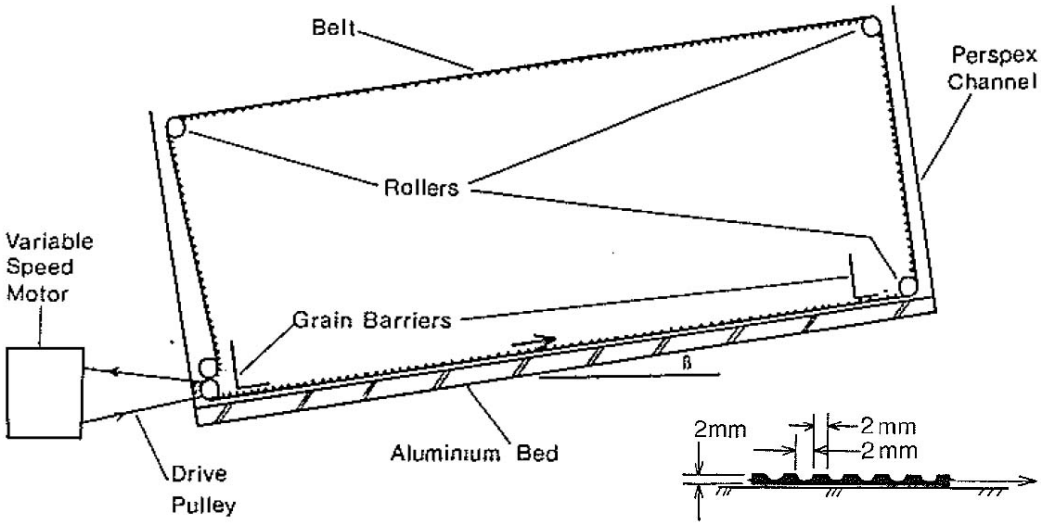

Fig. 6. Scheme of the moving-bed flume and detail of the corrugated nylon bed (Davies 1988).

The velocity distribution through the depth is similar in shape to the case of a fully-developed open channel flow over a erodible bed (Fig. 5), but there is slip at the bed and the mean flow velocity respect to the walls is zero. The only important difference from a traditional flume is that the wall friction in the moving-bed channel is directed downstream near the bed and

upstream away from the bed. The moving-bed flume can only be used to produce debris flow on a rigid bed, eliminating the possible analysis of erosion and deposition that would change the length of a wave. As a direct consequence, only steady waves can be studied.

The experimental flume is a 2 m long prismatic channel with a 50 mm wide rectangular section and transparent Perspex sidewalls. The moving bed is the grooved side of a corrugated nylon belt, with transverse grooves, 2 mm deep and 2 mm wide at 2 mm intervals (Fig. 6). The belt is supported by a system of smooth rollers and driven by a variable-speed electric motor. The fluid volume in the system is conserved by closing the ends of the flume; the loss of fluid from the belt rolling over the flume is prevented by Perspex strips. Grain barriers consisting of perforated steel plates prevent the jamming of particles in the lower rollers.

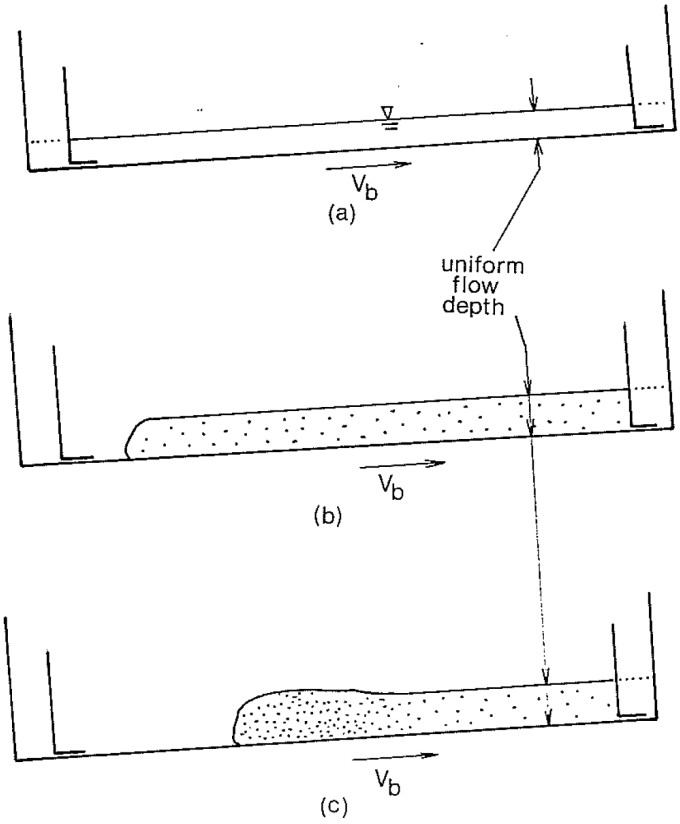

Fig. 7. The process of formation of the debris flow wave: a) uniform flow of water at a given slope and belt speed; b) the introduction of grains increases the flow resistance and, therefore, the flow depth to reach an equilibrium - if sufficient particles are added, an end wave appears in the channel; c) if the limit concentration of particles that can be carried by the uniform flow is exceeded, a bulbous wave of high concentration forms at the downstream end (Davies 1988).

The particles used in the experiments were dark green plastic cylinders, with a 4 mm diameter at the base and a height of 4 mm. About 10% of the grains were painted white and used as tracers. A small number of cylinders, 8 mm high with a base diameter of 8 mm, were introduced in the flow to study their behavior in a flow of smaller grains. The density of the particles was close to 1400 kg/m^3 and their maximum natural volume concentration was estimated to be 56%. The fluid used in most experiments was water at room temperature. The slope of the channel bed was adjusted within the range 5° to 19° and the belt speed varied between 0.25 m/s and 1.17 m/s. Rapid sequences of photos taken by a 35 mm motor-driven camera with a clock in the field of view were used to measure the belt speed, the channel slope, the wave size and shape, the grain concentrations, the local grain velocities, and the depth of the uniform flow. Video films were also used for tracking individual particle trajectories.

Stationary grain-water waves were easily obtained at any belt speed for slopes larger than 5°. For any belt speed and slope, uniform conditions could be established (Fig. 7a) upon the introduction of an adequate amount of water. For an excess volume of water, a pool forms at the downstream end of the flume, while uniform flow conditions persist upstream. On the contrary, if the water volume is too small, an end wave develops, while the flow upstream is still uniform. Starting from the condition represented in Fig. 7a, the introduction of particles increases the flow resistance and, therefore, the flow depth to reach equilibrium. As a consequence, if sufficient particles are added, an end wave appears in the channel (Fig. 7b). However, there is a limiting concentration of particles that can be carried by the uniform flow; if this is exceeded, a bulbous wave of high concentration forms at the downstream end (Fig. 7c).

The head wave produced in the moving-bed flume showed a series of consistent features: they consist mainly of a body, in which the flow is nearly uniform, that extends from a sharply curved front to a uniform sloping tail. The depth of the body increases as the belt speed increases, but it depends very weakly on the belt speed. The body depth is not affected by the total volume of particles, which induces an increase of the length of the body when it is increased. Finally, for bed slopes larger than 7°, the angle made by the surface of the tail with the horizontal is not affected by the bed slope, belt speed, or solids volume and assumes values of 7° ± 0.5°.

The analysis of particle velocity and granular concentration showed the largest concentration at the front of the debris flow and the smallest at the tail and at the free surface of the body. Relatively small values of the volume fraction were also observed within the body close to the bed, where the shear reaches the maximum values and the agitation of particles is enhanced. The shear reduces as the distance from the bed increases and, finally, the velocity becomes relatively uniform in the upper part of the body. As a main consequence, in the upper part of the front and of the body grains moved like a plug, with contact times of the order of one second. In this region, the free surface of the water was slightly below the top surface of the grains. The tail is different; it characterized by quite rapidly sheared grains close to the free surface and by the presence of water above them. Velocity observations from above did not show appreciable velocity variations across the channel width in any regions of the flow domain.

In some experiments, about 50 larger particles were inserted in the flume. When the maximum flow depth was thinner than about three times their diameter, the larger particles were concentrated at the front of the wave. For deeper flows, the large grains appeared almost uniformly distributed in all the regions of the flow in which the depth exceeded three times their size, except for the tail.

Flows on slopes above 5° showed either free surface instability in the form of roll waves or non-uniformity in the form of stationary waves. The latter phenomenon is typical of very dense flows, in which small local increases of the concentration can increase the flow resistance and reduce the speed, until more liquid and granular material accumulates from upslope, forcing the flow down slope again.

3. Modeling

3.1 Uniform flow

Although typical debris flow motion may be unsteady and develop through surges (Iverson 1997), the capability of a theory to reproduce the behavior of a granular-fluid mixture in well-controlled, uniform flow conditions seems a *sine qua non* requirement for its application to unsteady cases.

In debris flows, particle-particle-interactions, in instantaneous or enduring contact between the grains, and fluid-particle interactions determine the flow. The fluid transmits direct forces to the particles through drag and buoyancy and also influences the particle-particle interactions. The interactions between particles have been investigated in numerical simulations in dry granular flows (e.g., da Cruz, et al. 2005); their nature depends on the value of the particle concentration. At low concentrations in dilute flows, collisions dominate and the position and velocity of a single grain is uncorrelated with those of the others; at high concentration in dense flows, both correlated motions between the grains (Kumaran 2009) and possible long-lasting frictional contacts (da Cruz, et al. 2005) must be considered. Iverson (1997) indicates that the particle concentration in typical debris flows is between 0.4 and 0.6, so most of the flow is dense. Consequently, when modeling the global behavior of a debris flow, we ignore the possible presence of dilute regions in the flow. We focus on collisions because the experiments of Tubino and Lanzoni (1993), Armanini et al. (2005), and Larcher et al. (2007) indicate that collisions between particles are the dominant mechanism of momentum transport in large regions of the laboratory flows and because collisions seem to us to play an important role in Davies' (1988, 1990) experiments.

Kinetic theories (e.g., Garzo & Dufty 1999) have been successfully developed to derive constitutive relations from a characterization of the collisional interactions between particles; at low concentrations, these interactions are characterized by the coefficient of restitution, the ratio

of magnitudes of the relative velocities of two particles before and after a collision; this coefficient is less than unity in an inelastic collision. A characterization of the particle interactions at high-concentrations is far more complicated. Two approaches have been recently proposed that lead to relations between the stress and the motion in dense granular flows, at least in dry situations.

The French group GDR MiDi (2004) considers steady, dense, planar, shearing flows and focuses on the particle concentration c and ratio μ of the particle shear stress s and the particle pressure p. On the basis of dimensional analysis, they assert that in such dry flows, c and μ are unique functions of the inertial parameter $I \equiv |\dot{\gamma}| / (p / c)^{1/2}$, where $\dot{\gamma}$ is the strain rate, to be determined in numerical simulations or physical experiments. The inertial parameter is the ratio between time scales associated with particle motions parallel and perpendicular to the flow, respectively. Such a phenomenology lacks a constitutive relation for the particle pressure; it is determined through the momentum balance in the direction perpendicular to the flow (Jop et al. 2005; Cassar et al. 2005). However, with this determination of the pressure, the formulation permits easy solutions for the flow fields, because of the explicit relation between the particle shear stress and the strain rate.

Numerical simulations of shearing flows of circular disks (Mitarai and Nakanishi 2005) indicate that the main effect of the correlated motion between particles is to decrease the rate of collisional energy dissipation. This motivated Jenkins (2006, 2007) to propose a phenomenological correction to this term to be employed in existing kinetic theories. Dissipation in frictional contacts among the particles can also be incorporated using an effective restitution coefficient (Herbst et al. 2000). Consequently, this extended kinetic theory can be used to model more general dense, dry, granular flows.

In addition, Jenkins (2007) has shown that in regions of constant concentration away from boundaries in planar shearing flows, the extended kinetic theory and the GDR MiDi rheology can be linked, at least in flows in which collisions are the dominant means of momentum transfer. This provides a more physically-based justification of the use of the latter, which is simpler, when attempting to describe sufficiently thick flows. Also, it implies that the relation between the stress ratio on the inertial parameter in the simpler description should depend on the restitution coefficient.

When a fluid is present, the restitution coefficient, usually assumed constant in dry granular flows, is a function of the Stokes number (e.g., Zenit and Hunt 1998), a measure of particle inertia relative to the viscous force. For small enough values of the Stokes number, collisions are perfectly inelastic. In this case, a description of the flow based on purely collisional momentum transfer becomes suspect; although it has been suggested that in the GDR MiDi rheology, the transverse time scale in the inertial parameter associated with the pressure could be replaced with one associated with the viscous force (Cassar et al. 2005). Low values of the Stokes number are

typical of fine sediments. Larger sediments are characterized by low Stokes numbers only in a small region of vanishingly small velocity. Iverson (1997) indicates that in a typical debris flow, the content of fine sediments (silt and clay-sized grains) is less than 10% of the mass, the rest being composed of sand, gravel and larger boulders.

A two-phase model developed by Berzi and Jenkins (2008a, b; 2009) treats dense granular-fluid mixtures in which the inertia of cohesionless particles dominates fluid viscous forces in most of the flow and particle chains that do not span the flow may contribute to the transfer of momentum. The approach differs from previous treatments (e.g., Iverson 1997 2009, Pittman and Le 2005) in that it distinguishes between the depths and velocities of the particle and fluid phases. Here, we briefly summarize and further simplify a form of this theory that describes the uniform propagation of the granular-fluid mixture along an inclined bed. In this case, the bed is rigid and hence easy to locate, provided deposition does not occur.

When deposition does take place, a particle bed develops that is stationary, at least on the time-scale of laboratory experiments (Komatsu et al. 2001). The mechanics of the bed is different from that of the shearing flow. In the bed, particles form chains of contacts along the principal axes of compression and experience intermittent jumps out of the chains rather than continuous shearing. These chains provide a rate-independent resistance to shearing, but allow the bed to creep. Because the flow velocity at the bed is continuous and vanishes slowly with depth (Takahashi 1991; Armanini et al. 2005), the exact location of the erodible bed is difficult to specify.

We first apply the model to a steady, uniform flow in order to test against recent experiments carried out on such flows, which are discussed in Section 2. Details of the derivations are given by Berzi and Jenkins (2008b; 2009) and Jenkins and Berzi (2010) and Berzi et al. (2010a, b) discuss the further simplifications that we employ here.

We let ρ denote the fluid mass density, g the gravitational acceleration, σ the particle specific mass, d the particle diameter, η the fluid viscosity, U the fluid velocity, and u the particle velocity. The Reynolds number $R = \rho d(gd)^{1/2}/\eta$ is defined in terms of these. In what follows, we phrase the momentum balances and constitutive relations in terms of dimensionless variables, with lengths made dimensionless by d, velocities by $(gd)^{1/2}$, and stresses by $\rho\sigma gd$.

We take $z = 0$ to be the top of the grains, $z = h$ to be the position of either a rigid or erodible bed of inclination θ, and H to be the height of the water above the bed. The degree of saturation, H/h, is greater than unity in the over-saturated flows and less than unity in the under-saturated. In the latter case, a plug of extent ζ can be present in the upper part of the flow. These flows are again depicted in Fig. 8, together with a generic velocity profile for the particles.

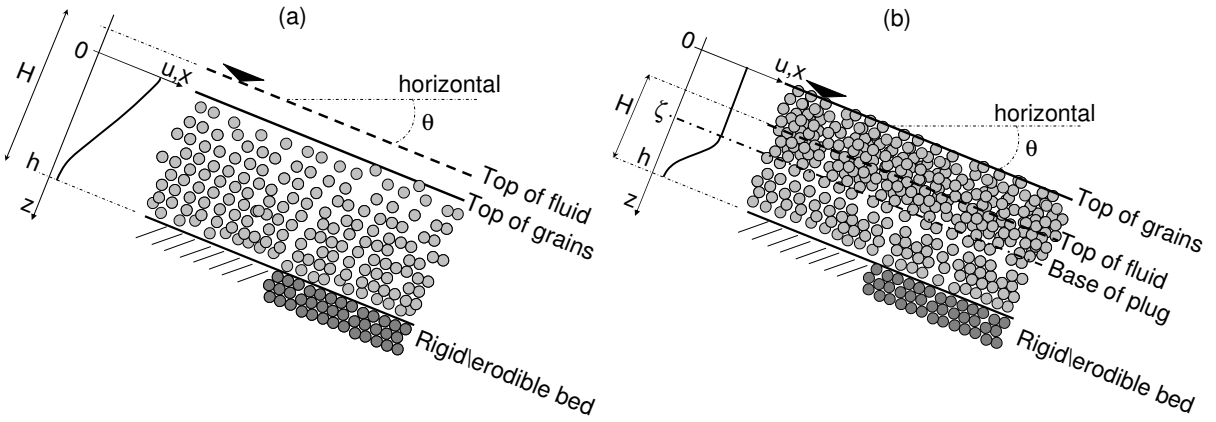

Fig. 8. Sketch of steady, (a) over- and (b) under-saturated, uniform flows over rigid and erodible beds.

We assume that it is possible to apply the GDR MiDi rheology and that the stress ratio and the concentration are approximately linear functions of the inertial parameter, as in numerical simulations of highly concentrated flows of disks (da Cruz et al. 2005),

$$\mu = \breve{\mu} + \chi I \tag{1}$$

and $c = \hat{c} - bI$, where $\breve{\mu}$ and $\hat{c}$ are the minimum stress ratio and the maximum concentration, respectively, and χ and b are material coefficients. In the flow configurations of Fig. 8, $|\dot{\gamma}| = -u'$ must be used in the definition of the inertial parameter; where here and in what follows, a prime indicates a derivative with respect to z. Also, we assume that the particle pressure, p, is the effective pressure, i.e. the total particle pressure minus the pore pressure, if present. The quantities $\breve{\mu}$ and $\hat{c}$ can be interpreted as the tangent of the angle of repose and the concentration at dense, random packing, respectively. As mentioned above, the relation between the stress ratio and the inertial parameter should depend on the value of the Stokes number, which varies with position in the flow. We assume that the linear rheology (1) also holds when an interstitial fluid is present; in this case, the coefficients $\breve{\mu}$, $\hat{c}$, χ and b incorporate the influence of the Stokes number. Consequently, the coefficients are not expected to be the same for dry granular flows and granular-fluid mixtures that consist of the same particles.

In the region in which both phases are present, the balances of fluid momentum transverse and parallel to the flow are

$$P' = \cos\theta / \sigma, \tag{2}$$

and

$$S' = (1-c)\sin\theta/\sigma - cC(U-u)/\sigma, \tag{3}$$

respectively, where P is the fluid pressure, S the fluid shear stress, and C is the dimensionless drag,

$$C \equiv \left(3|U-u|/10 + 18.3/R\right)/(1-c)^{3.1}, \tag{4}$$

introduced by Dallavalle (1943), with the concentration dependence suggested by Richardson and Zaki (1954). When an upper, clear fluid layer is present, the distribution of the fluid shear stress can be obtained from (3) with $c = 0$.

The balances of particle momentum transverse and parallel to the flow are

$$p' = (1-1/\sigma)c\cos\theta, \tag{5}$$

and

$$s' = c\sin\theta + cC(U-u)/\sigma, \tag{6}$$

respectively. The corresponding balances when an upper dry layer is present can be obtained from Eqs. (5) and (6) by letting σ become infinite. The fluid drag in Eq. (6) is, through the balance (3), the mechanism by which the weight of the fluid along the flow is transferred to the particles; this increases their mobility. Here, we ignore forces due to the lateral confinement of the flow. We will discuss this later.

As does Iverson (1997), in the mixture, we ignore the shear stress in the fluid relative to gravity and drag and, in the clear fluid layer, we assume that the turbulent mixing length is proportional to the thickness of the layer:

$$S = -k^2(H-h)^2|U'|U', \tag{7}$$

where $k = 0.20$, half the value of Karman's constant. Takahashi (1991) previously made use of Eq. (7), but also took into account the fluid shear stress in the mixture, assuming the mixing length there be proportional to the average distance between the particles. We call this the small-scale turbulence approximation to distinguish it from the approximation in which the mixing length is proportional to the fluid depth, H. Our earlier calculations (e.g., Berzi and Jenkins 2009) indicate that global quantities, such as the volume fluxes of particles and fluid and the angle of inclination of the free surface, are unaffected by the choice of the turbulence approximation.

Assuming that the concentration is approximately constant and at its maximum value, $c = \hat{c}$, and considering the surface at $z = 0$ as free of particle stress, it is possible to obtain the particle stress ratio, μ, as a function of z from the momentum balances (2), (3), (5) and (6) (Berzi and Jenkins 2009). The resulting expression is phrased in terms of two functions, α and β, of the degree of

saturation that permit a single expressions for a flow quantity to be written over the entire range of saturation: $\alpha = H/h$ in an under-saturated flow and unity otherwise, and $\beta = H/h$ in an over-saturated flow and unity otherwise. The result is

$$\mu = \frac{\left\{\hat{c}\sigma z + (1-\hat{c})\left[z - h(1-\alpha)\right]\right\}\sin\theta}{\left[\sigma z - z + h(1-\alpha)\right]\hat{c}\cos\theta} + \frac{h(\beta-1)\sin\theta}{\left[\sigma z - z + h(1-\alpha)\right]\hat{c}\cos\theta}. \tag{8}$$

Because of its relationship to the shear rate, the stress ratio can be seen as a measure of the mobility of the particles. This mobility is increased by the presence of the interstitial fluid: the apparent weight in the direction of the flow (the numerator of the first term on the right-hand side) increases due to drag; the apparent weight perpendicular to the flow (the denominator of both terms on the right-hand side) decreases due to buoyancy; and the shear stress associated with a layer of clear fluid above the mixture (the numerator of the last term on the right-hand side) forces particles in the direction of flow.

Where no fluid is present, Eq. (8) reduces to $\mu = \tan\theta$. Given that a shear rigidity develops when the stress ratio is below the tangent of the angle of repose, the upper dry layer is either totally sheared, when $\tan\theta > \breve{\mu}$, or there is a plug, when $\tan\theta \le \breve{\mu}$. Then, the base of the plug approximately coincides with the top of the fluid, in under-saturated flows. The distribution of the particle shear rate is obtained when the particle rheology (1) is employed in Eq. (8), with $I = -\sigma u' / \left\{\left[(\sigma-1)z + h(1-\alpha)\right]\cos\theta\right\}^{1/2}$ in the mixture layer and either $I = -u' / \left(z\cos\theta\right)^{1/2}$ or, if there is a plug, $I = 0$ in the dry layer. The distribution of the particle effective pressure is obtained from Eq. (5). Berzi et al. (2010a) give the distributions of the particle velocity in the mixture and in the upper dry layer when the turbulent fluid shear stress in the mixture is neglected, and Berzi and Jenkins (2009) provide those that result when the turbulent fluid shear stress in the mixture is taken into account.

For simplicity, we adopt the vanishing of the particle velocity as a boundary condition at the bed. Given that a slip velocity was observed for flows over rigid beds in experiments (Armanini et al. 2005) and that erodible beds creep (Komatsu et al. 2001), this boundary condition is another approximation in the model. With it, the distribution of the particle velocity can be more easily integrated to obtain the average particle velocities, u_m and u_{dry}, in the mixture and in the upper dry layer, respectively. With these, the total depth-averaged particle velocity, u_A, is

$$u_A = u_m\alpha + u_{dry}(1-\alpha), \tag{9}$$

and the particle volume flux per unit width, q, is $\hat{c}hu_A$. Upon employing the expressions of u_m and u_{dry} in Eq. (9), and assuming that the incline is mild, so that $\cos\theta \approx 1$ and $\sin\theta \approx \tan\theta$, we obtain the depth-averaged particle velocity as

$$u_A = \left(\lambda_1 \tan\theta - \lambda_2\right) h^{3/2}, \tag{10}$$

where the coefficients λ_1 and λ_2 are functions of σ, χ, $\breve{\mu}$, $\hat{c}$ and, through α and β, the degree of saturation. Expressions for them are given in Table 1.

The relation (10) between the average particle velocity, particle depth, and inclination is a reflection of the local rheology (1). It indicates that the global shear rate, u_A/h, of the particles, scaled with the square root of their transverse buoyant weight, varying with h, is proportional to the excess of the global stress ratio with respect to a yield. The global stress ratio is given in Eq. (8) as the sum of the drag and the flow component of the particle weight divided by their transverse buoyant weight; it is proportional to $\tan\theta$.

Table 1. Coefficients in Eq. (10) for the total depth-averaged particle velocity.

λ_1 when $\tan\theta \le \breve{\mu}$	$\frac{2}{15\chi\hat{c}\sigma^{1/2}(\sigma-1)^3}\left\{\left[(3\sigma-5+2\alpha)(\sigma-\alpha)^{3/2}-\sigma^{3/2}(3\sigma-5)(1-\alpha)^{5/2}\right](\hat{c}\sigma+1-\hat{c})\right.$ $\left.+5\left[(\sigma-3+2\alpha)(\sigma-\alpha)^{1/2}-\sigma^{1/2}(\sigma-3)(1-\alpha)^{3/2}\right]\left[(\sigma-1)(\beta-1)-\sigma(1-\alpha)\right]\right\}$
λ_1 when $\tan\theta > \breve{\mu}$	$\frac{2}{15\chi\hat{c}\sigma^{1/2}(\sigma-1)^3}\left\{\left[(3\sigma-5+2\alpha)(\sigma-\alpha)^{3/2}-\sigma^{3/2}(3\sigma-5)(1-\alpha)^{5/2}\right](\hat{c}\sigma+1-\hat{c})\right.$ $+5\left[(\sigma-3+2\alpha)(\sigma-\alpha)^{1/2}-\sigma^{1/2}(\sigma-3)(1-\alpha)^{3/2}\right]\left[(\sigma-1)(\beta-1)-\sigma(1-\alpha)\right]$ $\left.+3\hat{c}\sigma^{1/2}(\sigma-1)^3(1-\alpha)^{5/2}\right\}$
λ_2 when $\tan\theta \le \breve{\mu}$	$\frac{2}{15\chi\sigma^{1/2}(\sigma-1)^2}\left[(3\sigma-5+2\alpha)(\sigma-\alpha)^{3/2}-\sigma^{3/2}(3\sigma-5)(1-\alpha)^{5/2}\right]\breve{\mu}$
λ_2 when $\tan\theta > \breve{\mu}$	$\frac{2}{15\chi\sigma^{1/2}(\sigma-1)^2}\left[(3\sigma-5+2\alpha)(\sigma-\alpha)^{3/2}-\sigma^{3/2}(3\sigma-5)(1-\alpha)^{5/2}\right.$ $\left.+3\sigma^{1/2}(\sigma-1)^2(1-\alpha)^{5/2}\right]\breve{\mu}$

Because the theory is fully two-phase, it is possible to also determine the total depth-averaged fluid velocity in terms of the average fluid velocities in the mixture and in the upper clear fluid layer, U_m and U_{cm}, respectively:

$$U_A = \left[\alpha(1-\hat{c})U_m + (\beta-1)U_{cm}\right] / \left[\alpha(1-\hat{c}) + \beta - 1\right]. \tag{11}$$

The fluid volume flux per unit width, Q, is, then, $U_A\left[\alpha(1-\hat{c})h + (\beta-1)h\right]$.

With the drag balancing the component of the fluid weight along the flow, the difference between the fluid and the particle velocity obtained from Eq. (4) is an order of magnitude less than the particle velocity in the typical mixtures of water and granular material used in the laboratory experiments (Tubino and Lanzoni 1993; Armanini et al. 2005; Larcher et al. 2007). Therefore, in the steady, uniform flows, we take $U_m \approx u_m$; but retain the difference in the heights of the fluid and particle phases. We obtain the average fluid velocity in the upper, clear-fluid layer from successive integrations of Eq. (7) with the fluid shear stress given by Eq. (3) in the absence of particles. Finally, the total depth-averaged fluid velocity is

$$U_A = \left(\Lambda_1 \tan\theta - \Lambda_2\right) H^{3/2} + \Lambda_3 \left(\tan\theta\right)^{1/2} H^{1/2}, \tag{12}$$

where Λ_1, Λ_2 and Λ_3 are functions of σ, χ $\breve{\mu}$, $\hat{c}$, k and $\xi \equiv H/h$. Their expressions are given in Table 2.

Table 2. Coefficients in Eq. (12) for the total depth-averaged fluid velocity.

Λ_1	$\dfrac{2(1-\hat{c})}{15\xi^{3/2}\chi\hat{c}\sigma^{1/2}(\sigma-1)^3\left[\alpha(1-\hat{c})+\beta-1\right]}\Big\{\Big[(5\alpha\sigma-3\alpha-2\sigma)(\sigma-\alpha)^{3/2}+2\sigma^{5/2}(1-\alpha)^{5/2}$ $+5(\sigma-1)^{5/2}(\beta-1)\Big](\hat{c}\sigma+1-\hat{c})$ $+5\Big[(3\alpha\sigma-\alpha-2\sigma)(\sigma-\alpha)^{1/2}+2\sigma^{3/2}(1-\alpha)^{3/2}\Big]\Big[(\sigma-1)(\beta-1)-\sigma(1-\alpha)\Big]$ $+15(\beta-1)^2(\sigma-1)^{5/2}\Big\}$
Λ_2	$\dfrac{2(1-\hat{c})}{15\xi^{3/2}\chi\sigma^{1/2}(\sigma-1)^2\left[\alpha(1-\hat{c})+\beta-1\right]}\Big[(5\alpha\sigma-3\alpha-2\sigma)(\sigma-\alpha)^{3/2}+2\sigma^{5/2}(1-\alpha)^{5/2}+5(\sigma-1)^{5/2}(\beta-1)\Big]\breve{\mu}$
Λ_3	$\dfrac{2(\beta-1)^{3/2}}{5\xi^{1/2}k\left[\alpha(1-\hat{c})+\beta-1\right]}$

Eq. (12) indicates that the global shear rate, U_A/H, of the fluid is the sum of two contributions: the first is proportional to the global shear rate of the particles, as in Eq. (10); the second is proportional to $(\tan\theta/\mathrm{H})^{1/2}$, from the turbulence in the upper clear-fluid layer, as in the Darcy-Weissbach equation for turbulent fluids (Chow 1959).

The two expressions (11) and (12) for the total depth-averaged velocities relate the five variables u_A (or equivalently q), U_A (or equivalently Q), h, H, and $\tan\theta$. That is, in a steady, uniform, inclined flow of a granular-fluid mixture, three of these variables can be specified independently.

For example, we can specify the particle and fluid volume fluxes and the angle of inclination of the bed and determine the particle and fluid depths. There is, however, a key experimental observation for flows over an erodible bed (Armanini et al. 2005): the slope of the bed is not predetermined, as for the rigid bed, but is coupled with the volume fluxes.

In the above analysis, a no-slip condition was employed for both rigid and erodible beds. However, at an erodible bed and at a plug, it is more appropriate to prescribe the particle stress ratio as a yield condition. As in the particle rheology (1), this stress ratio is equal to the tangent of the angle of repose. However, Eq. (8) indicates that in moving from the free surface towards the bed in an under-saturated flow, the stress ratio increases monotonically, and that in a fully-saturated flow, it is constant. Consequently, the specification of a yield condition would lead to the impossibility of such flows over an erodible bed, in contrast to what is seen in the experiments of Armanini et al. (2005). In the context of the simple theory presented above, the resolution of this paradox is the inclusion, in an approximate way, of forces associated with the lateral confinement of the flow.

In a rectangular channel with frictional sidewalls a distance W apart and coefficient of sliding friction μ_w, the frictional resistance to particle flow increases from the free surface to the bed. It influences the value of the stress ratio at the bed and, therefore, the particle depth. The particle depth is obtained by introducing the frictional force in Eqs. (6) and (8) and taking $\mu = \breve{\mu}$ at $z = h$:

$$h = \frac{\left[\hat{c}\sigma + \alpha\left(1-\hat{c}\right) + \beta - 1\right]\tan\theta - \hat{c}\left(\sigma-\alpha\right)\breve{\mu}}{\hat{c}\left(\sigma-\alpha^2\right)\mu_w} W . \tag{13}$$

In an over-saturated flow, the presence of a lateral confinement is not required for yield at an erodible bed; in this case, the influence of the lateral confinement can be neglected in Eq. (8) if $\mu_w h / W \ll \breve{\mu}$, or when $\mu_w \sim \breve{\mu}$, if $h / W \ll 1$. In the latter case, Eq. (13) reduces to

$$\tan\theta = \hat{c}\left(\sigma-1\right)\breve{\mu} / \left[\hat{c}\left(\sigma-1\right) + \beta\right]. \tag{14}$$

Equation (13) or (14) provides an additional relation that reduces the number of unknowns for a flow over an erodible bed. Finally, it is worth noting that more fundamental theories than that outlined here, e.g. the extended kinetic theory of Jenkins (2006), also requires an additional boundary condition (e.g., Jenkins and Askari 1991) to determine the position of the bed.

The approximate theory outlined above and summarized in Eqs. (10) and (12) and, for a flow over an erodible bed, Eq. (13), is an advance over previous theoretical frameworks. For example, Takahashi's (1991) two-phase model for the uniform motion of over-saturated debris flows is based on a modified version of the dilatant model for the particle shear stresses in the inertial regime described by Bagnold (1954); it takes into account the difference in heights between the particles and the fluid, the dependence of the stress ratio on the particle concentration, and

incorporates the effects of the fluid turbulence. However, the theory is incomplete, because it cannot treat under-saturated debris flows. In addition, it does not incorporate yield of the particle phase that is present in many steady granular flows (Pouliquen 1999a; Cassar et al. 2005) and that is necessary to model the time-dependent transitions between statics and flow that are characteristic of surges (Iverson 1997).

Other two-phase models have been proposed by Iverson (1997, 2009) and Pitman and Le (2005); however, these do not allow for a degree of saturation different from unity and the resistance at the base of the flow is taken to be sliding friction. A consequence of the latter assumption is that the stress ratio at the bed, proportional to $\tan\theta$, is independent of the average velocity; this prevents an explanation of the experimentally observed dependence of the total depth-averaged particle velocity on the depth and slope in uniform flows (Tubino and Lanzoni 1993; Armanini et al. 2005). In the context of the present theory, these dependencies are captured in Eq. (10).

The superiority of two-phase models with respect to single-phase rheological models, in which the debris flow is modeled as a type of non-Newtonian fluid, has already been emphasized by Iverson (1997). Such models may be appropriate when the solid phase is composed of fine sediments, as in mud flows (e.g., Davies 1986).

In Table 3, we summarize the values of the four material parameters $\hat{c}$, $\breve{\mu}$, χ and μ_w, present in Eqs. (11), (12) and (13), that permit the reproduction of the experiments of Armanini et al. (2005) and Tubino and Lanzoni (1993) on steady, uniform flows of granular-fluid mixtures described in the previous section. For completeness, we also report in Table 3 the values of the parameters that apply to the uniform flow of dry glass spheres experimentally investigated by a (1999) and Jop et al. (2005), respectively.

As anticipated, the interstitial fluid affects the material parameters in the linear rheology (1); the minimum value of the stress ratio for glass spheres decreases to 0.34 from its value of 0.38 in dry conditions. Also, the particle diameter seems to play a role in the value of the minimum stress ratio: $\breve{\mu}$ is less for gravel A than for gravel B, according to the measurements of the angle of repose of the two materials in dry conditions made by Tubino and Lanzoni (1993).

In Fig. 9a, comparisons between the theory outlined above with the results of experiments for flows over erodible beds are shown as the flux ratio, $q/(q+Q)$, versus $\tan\theta$. An alternative would be to show the depths versus $\tan\theta$. We choose the flux ratio because it is only marginally affected by the relatively small variation of the fluid volume flux for the experiments reported in Table 3, although the relation between it and $\tan\theta$ is not unique for a particular set of parameters. Hence, the lines in Fig. 9a refer to theoretical results obtained keeping Q constant and equal to the mean of the experimental range in Table 3 and $q = \hat{c} u_A h$, with u_A and h provided by Eqs. (12) and (13). Also, we prefer to use the flux ratio because, as already mentioned, the position of the erodible bed, and therefore the evaluation of the particle and fluid heights above it, is still in question. In addition to this uncertainty in the location of the bed, the measurements

of the depths are local, in the sense that they are usually obtained through optical measurements of the flow field close to the sidewalls, and are, therefore, influenced by its presence (Armanini et al. 2005).

Table 3. Experimental conditions and fitted values of the material coefficients

Reference	Particles	Fluid	Geometry	q	Q	$\hat{c}$	$\bar{\mu}$	χ	μ_w
Jop et al. (2005)	Glass spheres (d = 5.0 mm, σ = 2.60)	No fluid	Rectangular flume (width = 1 to 30 cm) with glass sidewalls	1.0/65.0	-	0.60	0.38	0.60	0.22
Armanini et al. (2005)	Plastic cylinders (d = 3.7 mm, σ = 1.54)		Rectangular flume (width = 20 cm) with glass sidewalls	10.3/40.2	18.0/37.8	0.50	0.50	0.60	0.35
	Glass spheres (d = 3.0 mm, σ = 2.60)			5.1/47.6	15.5/22.3	0.60	0.34	0.60	0.19
Tubino and Lanzoni (1993)	Gravel A (d = 5.0 mm, σ = 2.65)	Water	Rectangular flume (width = 20 cm) with polycarbonate sidewalls	3.2/29.4	5.4/14.9	0.60	0.47	0.50	0.35
	Gravel B (d = 3.0 mm, σ = 2.65)			3.9/44.7	11.7/27.2	0.60	0.52	0.50	0.39

The theoretical curves show some distinctive features. There is an initial rapid growth of the flux ratio with $\tan\theta$ for low values of the free surface inclination; this corresponds to over-saturated flows. When the flux ratio reaches a value near $\hat{c}$, its increase with $\tan\theta$ is much less pronounced; this corresponds to under-saturated flows that involve a plug that extends up to the free surface. The kink in the curve corresponds to the saturated flow.

Armanini et al. (2005) report experiments on both over- and under-saturated flows and, as depicted in Fig. 9a, they show the features predicted by the theory. In contrast, Tubino and Lanzoni (1993) report on experiments only for saturated and over-saturated flows. Despite this, as seen in Fig. 9a, they do not observe the kink when the flux ratio is close to $\hat{c}$, set equal to 0.60 for both the glass spheres and the gravel - very close to the values measured by Tubino and Lanzoni (1993) in static packings. Assuming that the values of $\hat{c}$ are correct, values of the flux ratio so much higher than $\hat{c}$ in nearly saturated flows are possible only if the mean particle

velocity is much higher than the mean fluid velocity. Given that we expect the fluid be slightly faster than the particles in the layer where both phases are present, this is possible only if the flow is under-saturated and the upper dry layer is sheared. In the theory, the upper dry layer can be sheared only if $\tan\theta > \bar{\mu}$. However, for the experiments of Tubino and Lanzoni (1993), the calculated depth of this upper dry layer is less than one diameter. It is, therefore, likely that the particles there are not actually dry - an indication that capillarity can play an important role in laboratory experiments.

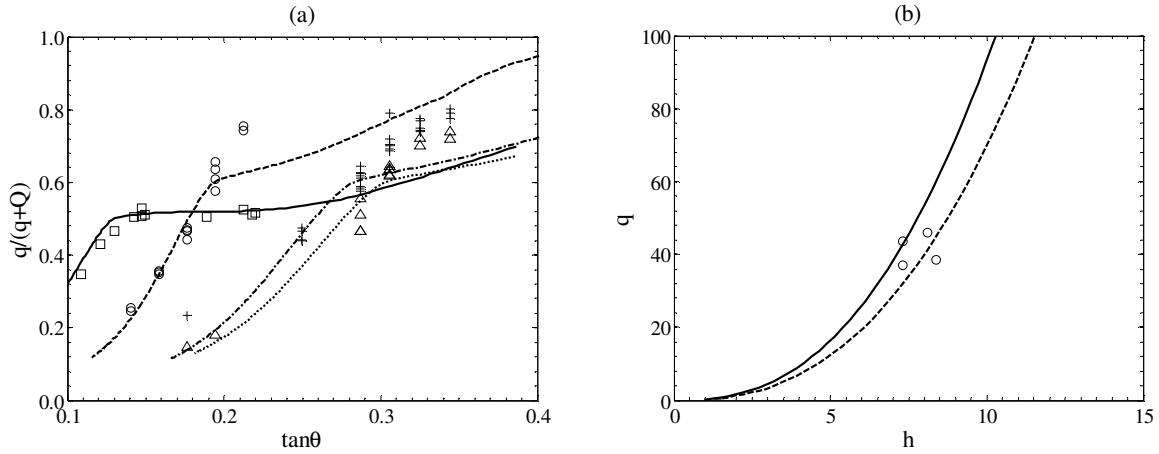

Fig. 9. (a) Experimental (symbols) and theoretical (lines) flux ratio versus tangent of the angle of inclination of the free surface for a mixture of water and: plastic cylinders (squares and solid line) flowing over erodible beds; glass spheres (circles and dashed line); gravel A (crosses and dot-dashed line); gravel B (triangles and dotted line). (b) Experimental (symbols) and theoretical (lines) particle volume flux versus particle depth for a nearly saturated mixture of water and plastic cylinders flowing over a rigid bed of: $\theta = 19°$ (dashed line); $\theta = 23°$ (solid line).

In Fig. 9b the comparison between the theory and the few available experiments on the nearly saturated flow of water and plastic cylinders over a rigid bed are depicted in terms of particle volume flux against particle depth, where, once again, $q = \hat{c} u_A h$, with u_A given by Eq. (12) and $\alpha = \beta = 1$ in the coefficients of Table 1. The theoretical curves are evaluated for the minimum and the maximum angles of inclination of the rigid beds investigated in the experiments. The agreement is, again, remarkable.

3.2 Non-uniform flow

We now turn to the analysis of the unsteady, non-uniform regime, considered by many (Iverson 1997, 2009; Hungr 2000) to be characteristic of debris flows. In unsteady, non-uniform motions, the debris flow may either erode or deposit granular material from or to the bed (e.g., and Young, 1998, Fraccarollo and Capart, 2002). The erosion and deposition rates are determined by the

transition between the flowing and the static states. Sufficiently dense static states are characterized by the fact that the granular material must expand in order to flow (Iverson 2009; Pailha and Pouliquen 2009). In the model described here, the transition between the flowing and the static state is controlled by the value of the particle stress ratio; hence, a relation between the local particle stress ratio and the dilation or compaction of the granular material near the transition must be provided. This would permit the description of the evolution of the interface between the flow and the bed. That is, flow initiates locally, somewhere in the static heap, and propagates into the material above. This is different from the approach of Iverson (2009) and Pailha and Pouliquen (2009), who describe the dilation and compaction as involving the entire granular material at once. Here, we defer the modelling of erosion and deposition and focus on unsteady flows over rigid beds at which particles are neither lost nor gained.

A sketch of the flow configuration and the coordinate system is depicted in Fig. 10. In contrast to Fig. 8, the origin of the Z-axis is at the rigid bed of inclination ϕ and the coordinate Z increases towards the free surface. The origin of the x-axis is taken to be somewhere upslope. The fluid and particle depths are now a function of position x and time t, so that in general $h(x,t)$ and $H(x,t)$ are not parallel to the rigid bed, as in uniform flows. When particle and fluid snouts are present as in the later analysis of steady waves over a rigid bed, we indicate their position by x^* and X^*, respectively.

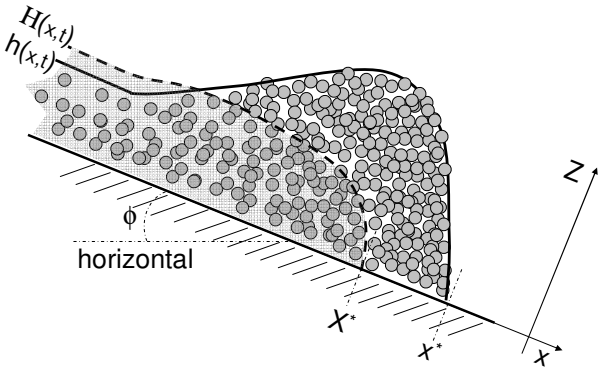

Fig. 10. Sketch of a non-uniform flow over a rigid bed.

The mass balance for the fluid is

$$\frac{\partial U}{\partial x}+\frac{\partial V}{\partial Z}=0, \tag{15a}$$

if $h \le Z \le \beta h,$ and

$$\frac{\partial(1-c)}{\partial t}+\frac{\partial\left[(1-c)U\right]}{\partial x}+\frac{\partial\left[(1-c)V\right]}{\partial Z}=0, \tag{15b}$$

if $0 \le Z \le \alpha h$; while that of the particles is

$$\frac{\partial c}{\partial t}+\frac{\partial(cu)}{\partial x}+\frac{\partial(cv)}{\partial Z}=0, \tag{16}$$

where V and v are the fluid and the particle velocities in the Z-direction.

When the slope of the rigid bed is assumed to be mild, $\sin\phi \approx \tan\phi$, and the longitudinal momentum balance for the fluid may be written as

$$\frac{1}{\sigma}\left(\frac{\partial U}{\partial t}+U\frac{\partial U}{\partial x}+V\frac{\partial U}{\partial Z}\right)=\frac{1}{\sigma}\tan\phi+\frac{\partial S}{\partial Z}-\frac{\partial P}{\partial x}, \tag{17a}$$

if $h \le Z \le \beta h$; and

$$\frac{1-c}{\sigma}\left(\frac{\partial U}{\partial t}+U\frac{\partial U}{\partial x}+V\frac{\partial U}{\partial Z}\right)=\frac{1-c}{\sigma}\tan\phi-\frac{c}{\sigma}C(U-u)+\frac{\partial S}{\partial Z}-\frac{\partial\left[(1-c)P\right]}{\partial x}-P\frac{\partial c}{\partial x}, \tag{17b}$$

if $0 \le Z \le \alpha h$, where the term involving the derivative of concentration along the flow accounts for the buoyancy of the particles (Drew and Passman 1999). The present treatment of the buoyancy is consistent with the deeper analysis performed by Pitman and Le (2005). Similarly, the longitudinal momentum balance for the particles is

$$c\left(\frac{\partial u}{\partial t}+u\frac{\partial u}{\partial x}+v\frac{\partial u}{\partial Z}\right)=c\tan\phi+\frac{\partial s}{\partial Z}-\frac{\partial p}{\partial x}, \tag{18a}$$

if $\alpha h \le Z \le h$, and

$$c\left(\frac{\partial u}{\partial t}+u\frac{\partial u}{\partial x}+v\frac{\partial u}{\partial Z}\right)=c\tan\phi+\frac{1}{\sigma}cC(U-u)+\frac{\partial s}{\partial Z}-\frac{\partial(p+cP)}{\partial x}+P\frac{\partial c}{\partial x}, \tag{18b}$$

if $0 \le Z \le \alpha h$, where $p+cP$ is the total particle pressure, assumed to be isotropic. The latter assumption is in contrast to that employed in models that originate in soil mechanics (Savage and Hutter 1989; Iverson 1997, 2009). In these, the ratio of the particle normal stress parallel and perpendicular to the flow is taken to be a coefficient different from unity. The determination of this earth pressure coefficient is based on the assumption that the granular material internal to the flow is at yield (Savage and Hutter 1989). In our model, this condition holds only at the erodible bed and at the plug. In the absence of experimental evidence of anisotropic normal stresses in the flow (cf., Hungr 1995), we assume isotropy.

The mass balances (15) and (16) are averaged through the total depth of the flow over a rigid bed, assuming that the particle concentration is constant and equal to $\hat{c}$, with the depth-averaged particle concentration through H denoted by c_A:

$$\frac{\partial\left[\left(1-c_A\right)H\right]}{\partial \mathrm{t}}+\frac{\partial\left[\left(1-c_A\right)HU_A\right]}{\partial \mathrm{x}}=0; \tag{19}$$

and

$$\frac{\partial h}{\partial \mathrm{t}}+\frac{\partial\left(hu_A\right)}{\partial \mathrm{x}}=0, \tag{20}$$

where

$$\left(1-c_A\right)H=\left[\alpha\left(1-\hat{c}\right)+\beta-1\right]h. \tag{21}$$

Similarly, the momentum balances (17a) and (17b) are averaged through the depth and, in the resulting equations, the terms that involve the sum of shear stress at the bed and the average drag force in the direction of the flow is replaced by its value in a steady, uniform flow. This value, denoted by J, is obtained from Eq. (12) by solving for the tangent of the angle of inclination in the steady, uniform flow:

$$J=\left\{\frac{-\Lambda_3+\left[{\Lambda_3}^2+4\Lambda_1\left(\Lambda_2H^2+U_AH^{1/2}\right)\right]^{1/2}}{2\Lambda_1H}\right\}^2. \tag{22}$$

With this, the depth-averaged equation is

$$\frac{\partial\left[\left(1-c_A\right)HU_A\right]}{\partial t}+\frac{\partial\left[\left(1-c_A\right)H{U_A}^2\right]}{\partial x}=\left(1-c_A\right)H\left(\tan\phi-J-\frac{\partial H}{\partial x}\right). \tag{23}$$

In the same way, the depth-averaged equation for the particles is

$$\frac{\partial\left(hu_A\right)}{\partial t}+\frac{\partial\left(h{u_A}^2\right)}{\partial x}=h\left\{\tan\phi-j-\frac{\partial h}{\partial x}-\frac{\alpha}{\sigma}\frac{\partial\left[\left(\beta-1\right)h\right]}{\partial x}\right\}, \tag{24}$$

where

$$j=\frac{1}{\lambda_1}\frac{u_A}{h^{3/2}}+\frac{\lambda_2}{\lambda_1}. \tag{25}$$

The resulting model consists of a system of four partial differential equations in the variables $(1-c_A)H$, h and the two momenta $(1-c_A)HU_A$ and hu_A. In obtaining this system, we made multiple use

of Leibniz's rule for the derivative of an integral, the kinematic boundary condition at a material surface, the rigidity of the bed, and the jump condition at the interface between the clear fluid and the mixture layer (for more details, see Berzi and Jenkins 2009). In hydraulics (e.g., Chow, 1959), the quantities J and j are called friction slopes because they characterize the resistance of the flow to the force associated with the inclination in steady, fully developed circumstances. The solution of the system (19) through (25) requires initial as well as boundary conditions. A natural choice for the latter may be the particle and fluid upstream volume fluxes and the particle and fluid heights either upstream or downstream, depending on the mathematical nature of the system (19)-(25) (for a discussion about the hyperbolicity of a similar two-phase mathematical model in which, however, there is no difference in the particle and fluid heights, see Pitman and Le 2005).

The mathematical model is based on the assumption that the distribution of fluid pressure is hydrostatic and that the particle effective pressure balances the buoyant weight of the particle phase. This is true when the transverse drag force and the inertia associated with the transverse acceleration in the Z-momentum balances are neglected. Using scaling arguments, Pitman and Le (2005) show that these terms are of the same order of magnitude as the ratio between the flow depth and its length; consequently, in the context of a shallow-water theory, their neglect is permitted. However, Iverson (1997, 2009) has focused attention on the possibility that because of the drag of the particles on the transverse flow of the fluid, the distribution of fluid pressure is not hydrostatic. This could influence the mobility of debris flows by reducing the effective particle pressure. The arguments that explore this possibility typically disregard the inertia of the transverse acceleration - an inconsistency in the depth-averaged mathematical modelling. Ignoring this, the retention of the transverse drag force in the Z-momentum balances leads to the additional terms $-\partial D/\partial x$ and $+\partial D/\partial x$ on the right-hand side of the depth-averaged momentum balances for the fluid and the particles, respectively, where

$$D = \int_0^{\alpha h} \int_\zeta^{\alpha h} \hat{c} C \left(V - v \right) / \sigma \, dZ d\zeta \tag{26}$$

is the average transverse drag force.

To evaluate this term, Iverson (1997, 2009) must assume a fluid pressure distribution, because he does not allow for the fluid and particle heights to be different. In the context of our model, D can be evaluated in a more natural way as $D \approx \hat{c} C \left(\alpha h \right)^2 \left(V_A - v_A \right) / \left(2\sigma \right)$, where V_A and v_A are the average velocities of the fluid and the particles along Z. We assume that V_A and v_A are approximately constant and equal to half the values of the Z-component of the fluid and particle velocity at $Z = H$ and $Z = h$, respectively. The latter are material boundaries, so that $V\big|_{Z=H} = \partial H/\partial t + U\big|_{Z=H} \partial H/\partial x$ and $v\big|_{Z=H} = \partial h/\partial t + u\big|_{Z=H} \partial h/\partial x$. With the further approximations $U\big|_{Z=H} = 2U_A$ and $u\big|_{Z=H} = 2u_A$, the average transverse drag force is

$$D \approx \frac{\hat{c}C(\alpha h)^2}{2\sigma}\left[\frac{1}{2}\frac{\partial(H-h)}{\partial t}+U_A\frac{\partial H}{\partial x}-u_A\frac{\partial h}{\partial x}\right]. \tag{27}$$

Eq. (27) permits a quantitative *a posteriori* evaluation of the influence of the transverse drag force on the debris flow motion. Its introduction into the mathematical model, although possible, would require a more sophisticated numerical method than that adopted here for the determination of steady, non-uniform solutions to the system.

As described in Section 2, there are only a few laboratory experiments on non-uniform debris flows to be used to test the mathematical model outlined above. Among them, those performed by Davies (1988, 1990) in steady conditions are the most carefully described, and seem to possess some features in common with natural debris flows. Consequently, they are a realistic test of the present theory for its possible practical applications.

A wave that translates along an incline without changing its longitudinal profile is called a uniformly progressive wave (e.g., Chow 1959). The wave is characterized by the fact that any moving material element of extent dx in Fig. 10 has a constant depth-averaged velocity. Uniformly progressive waves have already been analysed by Pouliquen (1999b) for dry granular flows and by Hungr (2000), using a single-phase model for granular-fluid mixtures. Here, we emphasize what are the implications of letting the heights of the fluid and the particles differ, as in the theory of Berzi and Jenkins (2009).

If, in Fig. 10, the coordinate system is in translation with the common depth-averaged velocity, both the particle and the fluid depth are functions only of x, and x^* and X^* are constants. We assume, as in Davies' (1988) experiments, that the wave front is dry, so that $X^* < x^*$. With the particle and fluid depth-averaged velocities equal and constant at every x, the fluid and particle x-momentum balances reduce to

$$\frac{\partial \mathrm{H}}{\partial \mathrm{x}} = \tan\phi - \mathrm{J}, \tag{28}$$

and,

$$\frac{\partial \mathrm{h}}{\partial \mathrm{x}} + \frac{\alpha}{\sigma}\frac{\partial\left[(\beta-1)\mathrm{h}\right]}{\partial \mathrm{x}} = \tan\phi - \mathrm{j}, \tag{29}$$

respectively. Solutions of the two ordinary differential equations (28) and (29) provide the evolution of the depths $h(x)$ and $H(x)$ once the slope of the rigid bed, $\tan\phi$, the common value of the average velocities, $u_A = U_A$, for the determination of the friction slopes, and two boundary conditions, associated with the vanishing of the particle and fluid depths at the snouts, are specified.

In the dry front, the evolution of the particle depth is governed by Eq. (29), with $\beta = 1$, $\alpha = 0$ and $j = \breve{\mu} + 5\chi u_A / \left(2h^{3/2}\right)$ (Berzi and Jenkins 2009). It is easy to show (Pouliquen 1999b) that from a dry front, the particle depth tends monotonically to the value that is the solution of the uniform dry flow, $j = \tan\phi$. In the context of the model, this value is positive only if the angle of inclination of the rigid bed is greater than the angle of repose of the granular material. For the plastic cylinders used by Armanini et al. (2005), which are similar, although heavier, than those of Davies (1988), this implies that a dry granular front can be present only at angles of inclination of the bed greater than, roughly, 26° (from Table 3). However, Davies (1988, 1990) observed the presence of a dry front at angles of inclination as low as 10°.

We note that in Davies' (1990) experiments, the dense granular-fluid flow developed over a thin collisional basal layer (Jenkins and Askari 1999); hence, both the use of the GDR MiDi rheology and the assumption of a zero slip velocity at the bed are inappropriate. Despite this, we will show that the qualitative behaviour of the steady wave at angles of inclination of the rigid bed greater than 26° is in accordance with the observations reported by Davies (1988, 1990). Also, we will show that at least some of the quantitative predictions of the theory of Berzi and Jenkins (2009) are in good agreement with these experiments.

As do Berzi and Jenkins (2009), we employ a fourth-order Runge-Kutta method to solve the two differential equations (28) and (29). The inclination of the rigid bed, the depth-averaged constant velocity, the position, x^*, and the longitudinal extension, $x^* - X^*$, of the dry front are the input parameters. The specification of the latter two parameters is equivalent to the specification of the total volume per unit width of the fluid and particles between the snout and the origin of the x-axis (Berzi and Jenkins 2009); these are the parameters controlled in Davies' (1988, 1990) experiments. At each step of the integration, J and j, which depend on the depth-averaged velocities and the fluid and particle depths, are evaluated using Eqs. (22) and (25).

Here, as in Berzi and Jenkins (2009), we present the results for the steady, non-uniform flow of a mixture of water and the plastic cylinders used by Armanini et al. (2005), with the properties summarized in Table 3. As already mentioned, Davies (1988, 1990) made use of similar particles (see Section 2) in his moving-bed apparatus. As explained by Davies, fixing the belt velocity in the moving-bed apparatus is equivalent to fixing the depth-averaged velocities $u_A = U_A$ in the laboratory frame of reference.

In Fig. 11, we show depths that result from the numerical solution of Eqs. (28) and (29) for $\phi = 30°$. They exhibit distinctive features of debris flows observed both in the laboratory (Davies 1988) and in nature (Takahashi 1991, Iverson 1997): there is a front (head) in which the particle depth increases upslope, a body characterized by an approximately constant depth, and a tail where the depth diminishes (Fig. 11a). Fig. 11a shows that the wave bulges at the front because the depth of the uniform dry granular flow is greater than the depth of the uniform granular-fluid flow; the particle depth initially seeks the former, but eventually asymptotes to the latter. As

observed by Davies (1988), increasing the longitudinal extension of the dry front causes the length of the body to increase, without substantially affecting the shape of the front or the tail. Fig. 11b shows that an increase of the depth-averaged velocity causes an increase in the maximum height of the wave and a decrease in the length of the body; once again, this is in accordance with Davies' (1988, 1990) observations. A similar behaviour can be obtained by decreasing the inclination of the rigid bed (Berzi and Jenkins 2009).

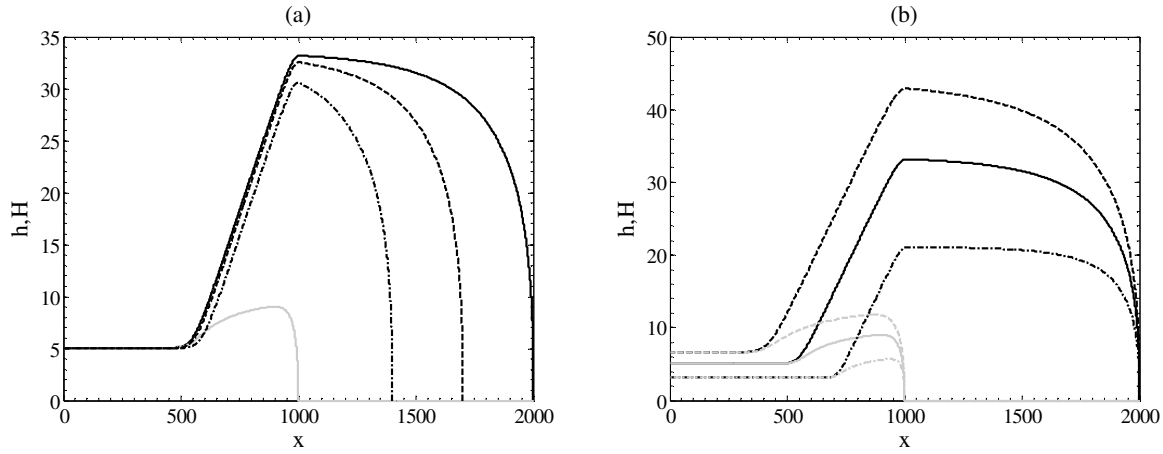

Fig. 11. (a) Particle depth (black lines) versus position for a granular-fluid wave over a rigid bed with $\phi = 30°$ and $u_A = U_A = 10$, for $x^* - X^* = 400$ (dot-dashed line), $x^* - X^* = 700$ (dashed line), and $x^* - X^* = 1000$ (solid line). The fluid depth versus position, substantially independent of the longitudinal extension of the dry front, is represented by the gray solid line. (b) Particle depth (black lines) and fluid depth (gray lines) versus position for a granular-fluid wave over a rigid, bumpy bed with $\phi = 30°$ and $x^* - X^* = 1000$, for $u_A = U_A = 5$ (dot-dashed lines), $u_A = U_A = 10$ (solid lines) and $u_A = U_A = 15$ (dashed lines).

In Fig. 12, the depths of two saturated flows are shown as a function of x for two experiments Davies (1990) performed at angles of inclination of the rigid beds less than the angle of repose of the granular material. Here, we abandon the idea of reproducing the front and the body of the wave that Davies' observations indicate are dry and under-saturated. As already mentioned, at these angles, an approach that incorporates a collisional basal layer is required (Jenkins and Askari 1999). Nevertheless, if we adopt as upstream conditions the common depths h and H, the theory can reproduce the behaviour of the tail.

The predictions for steady, non-uniform flows suggest that two important features of debris flows, observed in the field, can be explained in the contest of the present two-phase approach. These are the bulbous shape of the front and the fact, indicated by well-controlled measurements

(Iverson 1997), that it is dry. The bulging of the wave can be reproduced without appeal to either an artificially imposed longitudinal variation of the solid concentration, as in Hungr (2000) or the necessity of size-segregation (e.g., Gray and Thornton 2005), although segregation by size certainly occurs at the front. Recent advances in modelling particle segregation in binary mixtures are reported in the next sub-section. We note that the formation of lateral levees can also be interpreted as the propagation of dry, bulbous fronts of a mixture of grains and fluid.

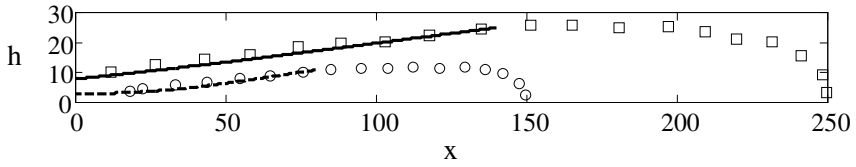

Fig. 12. Experimental (symbols, after Davies 1990) and theoretical (lines) flow depth versus position for a granular-fluid wave over a rigid bed with $u_A = U_A = 1.84$, for $\phi = 15°$ (circles and dashed line), and $\phi = 12.5°$ (squares and solid line).

Finally, it is worth noting that bulging in debris flows has been associated by Iverson (1997) with roll waves - surface instabilities typical of shallow water. Indeed, unsteadiness and intermittency are often observed in granular-fluid mixtures, even when a steady, uniform flow might be expected. Such instabilities typically occur when the particle volume flux exceeds a certain threshold, at a given total volume flux. Roll waves manifest themselves in many flows (Balmforth and Mandre 2004 and references therein), including dry granular flows on inclines (Forterre and Pouliquen 2003). As in the latter situation, it is likely that a linear stability analysis carried out on the system (19) through (25) would provide a limiting value for the particle volume flux, at fixed fluid volume flux for which a stable uniform flow is possible.

3.3 Size-segregation

We next outline a kinetic theory for segregation of particles that differ by size and/or mass in a uniform, fully saturated binary mixture of particles in which the particle-particle interactions are dominated by collisions. We indicate the similarities and differences between this theory and existing phenomenological theories (Lun and Savage 1988, Gray and Thornton 2005, Gray and Chugunov 2006, Thornton, et al. 2006, Thornton and Gray 2008) for segregation in dry flows. More details of the derivation in the case of dry flows may be found in Larcher & Jenkins (2010). We focus the attention on the case where one granular species is dilute in the other and determine the equation that describes the time and space evolution of the concentration of the

dilute species in a steady, inclined flow of a dense granular-fluid mixture. In this section, we first work in terms of dimensional quantities and then phrase the final equations in dimensionless form. We employ the coordinate system of Fig. 10.

We consider nearly elastic spherical particles of masses m^A and m^B, radii r^A and r^B, velocities $\boldsymbol{u}^A$ and $\boldsymbol{u}^B$, number densities n^A and n^B, and concentrations c^A and c^B, with $m^{AB} = m^A + m^B$, $r^{AB} = r^A + r^B$, $n = n^A + n^B$, and $c = c^A + c^B$. The mass density ρ^A for species A is defined as $\rho^A = m^A n^A = \rho^{sA} c^A$, where ρ^{sA} is the mass density of the material constituting species A; its concentration and the number density are related by $c^A = 4\pi \left(r^A \right)^3 n^A / 3$. Similar relations can be written for species B.

As in the continuum mixture theory just discussed, the kinetic theory of mixtures employs mass and momentum balances for each granular species. The momentum balances involve stress tensors, a force of interaction between species, and external forces. The mass and momentum balances for the particles are the sums of those for the two granular species; they are phrased in terms of the particle mass density and a mass-averaged particle velocity. Segregation is described using the difference of the mass balances with a flux term that results from a weighted difference of the momentum balances with the inertia associated with species velocities relative to the mass-averaged particle velocity neglected and all stresses are taken to be pressures. The granular temperature that appears in the expressions for the particle pressures and the interaction force is the average kinetic energy of the velocity fluctuations of the particles.

The mass balance for species A is:

$$\frac{\partial \rho^A}{\partial t} + \frac{\partial}{\partial x_\alpha} \left(\rho^A \mathrm{u}_\alpha^A \right) = 0, \tag{30}$$

where $\alpha = 1$ and 2, with $x_1 = x$ and $x_2 = Z$. The particle mass density ρ is $\rho = \rho^A + \rho^B$ and the particle mass-center velocity $\boldsymbol{u}$ is $\rho \boldsymbol{u} = \rho^A \boldsymbol{u}^A + \rho^B \boldsymbol{u}^B$; Then, for example, the diffusion velocity $\boldsymbol{v}^A$ of species A is defined as the difference between the velocity $\boldsymbol{u}^A$ of the species and the mass-center velocity $\boldsymbol{u}$: $\boldsymbol{v}^A = \boldsymbol{u}^A - \boldsymbol{u}$, with $\rho^A \boldsymbol{v}^A + \rho^B \boldsymbol{v}^B = 0$. The mass balance for species A can be written in terms of these quantities as

$$\frac{\partial \ln n^A}{\partial t} + \frac{\partial u_\alpha}{\partial x_\alpha} + u_\alpha \frac{\partial \ln n^A}{\partial x_\alpha} + \frac{\partial v_\alpha^A}{\partial x_\alpha} + v_\alpha^A \frac{\partial \ln n^A}{\partial x_\alpha} = 0. \tag{31}$$

The mass balance for species B can be written in a similar way. Taking their difference results in

$$\frac{\partial}{\partial t} \left(\ln \frac{n^B}{n^A} \right) + u_\alpha \frac{\partial}{\partial x_\alpha} \left(\ln \frac{n^B}{n^A} \right) + \frac{\partial}{\partial x_\alpha} \left(v_\alpha^B - v_\alpha^A \right) + v_\alpha^B \frac{\partial \ln n^B}{\partial x_\alpha} - v_\alpha^A \frac{\partial \ln n^A}{\partial x_\alpha} = 0. \tag{32}$$

When the convective terms associated with the diffusion velocities are neglected, this becomes

$$\frac{\partial}{\partial t}\left(\ln\frac{n^B}{n^A}\right)+u_\alpha\frac{\partial}{\partial x_\alpha}\left(\ln\frac{n^B}{n^A}\right)+\frac{\partial}{\partial x_\alpha}\left(v_\alpha^B-v_\alpha^A\right)=0. \tag{33}$$

This equation serves to describe the segregation of the two particle species, once the difference in diffusion velocities is determined using the particle momentum balances.

The momentum balance for species *A* is

$$\frac{\partial u_\alpha^A}{\partial t}+u_\beta^A\frac{\partial u_\alpha^A}{\partial x_\beta}=\frac{1}{\rho^A}\frac{\partial t_{\alpha\beta}^A}{\partial x_\beta}+\frac{1}{m^A}F_\alpha^A+\frac{1}{\rho^A}\Phi_\alpha^A, \tag{34}$$

where $\beta=1$ and 2, $\boldsymbol{t}^A$ is the effective stress, $\boldsymbol{F}^A$ is the external force, including fluid drag, on a particle, and $\boldsymbol{\Phi}^A$ is the rate of momentum exchange between the two granular species. The momentum balance for species *B* can be written in a similar way with $\boldsymbol{\Phi}^B=-\boldsymbol{\Phi}^A$. Here, for the rate of momentum exchange, we employ a simple form derived by Jenkins & Mancini (1997):

$$\Phi_\alpha^A=\frac{2\pi}{3}g^{AB}\left(r^{AB}\right)^3n^An^BT\left\{\frac{m^B-m^A}{m^{AB}}\frac{\partial\ln T}{\partial x_\alpha}-\frac{\partial}{\partial x_\alpha}\left(\ln\frac{n^B}{n^A}\right)+\frac{4}{r^{AB}}\left(\frac{2m^Am^B}{\pi m^{AB}T}\right)^{1/2}\left(v_\alpha^B-v_\alpha^A\right)\right\}, \tag{35}$$

in which g^{AB} is the radial distribution function of species *A* and *B* and *T* is the granular temperature of the particles.

The weighted difference of the two particle momentum balances is, with the neglect of the inertia associated with the diffusion velocities and when all stresses are taken to be pressures,

$$0=-\rho^B\frac{\partial\pi^A}{\partial x_\alpha}+\rho^A\frac{\partial\pi^B}{\partial x_\alpha}+\rho^A\rho^B\left(\frac{F_\alpha^A}{m^A}-\frac{F_\alpha^B}{m^B}\right)+\left(\rho^A+\rho^B\right)\Phi_\alpha^A. \tag{36}$$

where π^A and π^B are the partial pressures. Jenkins & Yoon (2002) show that when species *B* is dilute in dense species *A*, $n^B/\,n^A\ll1$, the partial pressures simplify to

$$\pi^A=\frac{16\pi}{3}\left(n^A\right)^2g^{AA}\left(r^A\right)^3T\ \text{ and }\ \pi^B=\frac{2\pi}{3}n^An^Bg^{AB}\left(r^{AB}\right)^3T, \tag{37}$$

where g^{AA} and g^{AB} are given as functions of the radii ratio and the particle concentration by

$$g^{AA}=\frac{(2-c)}{2(1-c)^3}\ \text{ and }\ g^{AB}=\frac{\left[(1-c)(1+r^A/r^B)+c\right]\left[(1-c)(1+r^A/r^B)+2c\right]}{(1+r^A/r^B)^2(1-c)^3}. \tag{38}$$

For the purpose of segregation, the particle momentum balance is approximated by

$$0 = -\frac{\partial}{\partial x_\alpha}\left(\pi^A + \pi^B\right) + \frac{\rho^A}{m^A} F_\alpha^A + \frac{\rho^B}{m^B} F_\alpha^B . \tag{39}$$

Then, upon employing this to eliminate the gradient of π^A from Eq. (36) and solving the result for $\boldsymbol{v}^B - \boldsymbol{v}^A$, we have

$$\begin{aligned} v_\alpha^B - v_\alpha^A = {} & \frac{3}{8\pi} \frac{1}{g^{AB}\left(r^{AB}\right)^2 n^A T} \left(\frac{\pi m^{AB} T}{2 m^A m^B}\right)^{1/2} \\ & \times \left\{ F_\alpha^B - \frac{1}{n^B}\frac{\partial \pi^B}{\partial x_\alpha} + \frac{2\pi}{3} g^{AB}\left(r^{AB}\right)^3 n^A T \left[\frac{m^B - m^A}{m^{AB}} \frac{\partial \ln T}{\partial x_\alpha} - \frac{\partial}{\partial x_\alpha}\left(\ln \frac{n^B}{n^A}\right)\right]\right\}. \end{aligned} \tag{40}$$

As in the case of a dense debris flow with a single granular species, we assume that the particle concentration, equal here at lowest order to that of species *A*, is constant. Then, Eq. (40) indicates the motion of *B* with respect to *A* is influenced by gravity, fluid drag, gradients of the particle velocity fluctuations, and spatial inhomogeneity in its number density. In order to say more about the relative magnitude of these terms, we must characterize the external force and the temperature and velocity fields of the mixture.

When the fluid shear stress in the dimensional form of Eq. (4) is neglected, fluid drag is balanced by the component of the weight of the fluid in the flow direction. Then, at lowest order in n^B/n^A, the specific mass, concentration, and velocity of *A* are those of the particles, and

$$n^A F_x^A = \rho^A g \sin\phi + \rho^A \frac{C\left(U-u\right)}{\sigma r^{AB}} = \rho^A \left[\frac{1 + c(\sigma - 1)}{\sigma c}\right] g \sin\phi \tag{41}$$

and

$$n^A F_Z^A = -\rho^A \left(\frac{\sigma - 1}{\sigma}\right) g \cos\phi ; \tag{42}$$

the components of $\boldsymbol{F}^B$ can be obtained from these by replacing *A* with *B*. These equations indicate how the influence of gravity on the particles is modified by fluid drag and buoyancy, respectively. We employ these modifications in the profiles of temperature and particle velocity determined by Jenkins and Berzi (2010) for a steady, uniform, dense, dry, inclined flow of identical spheres. When species *B* is dilute in a steady, uniform, inclined flow of a fully saturated mixture of a dense species *A* and water, these become:

$$T(Z) = \frac{1}{4} m^A \frac{(H - Z)}{\hat{c}\hat{g}^{AA}} \frac{\sigma - 1}{\sigma} g \cos\phi , \tag{43}$$

where $\hat{g}^{AA}$ is evaluated at $\hat{c}$, and

$$u(Z)=\left[\frac{\pi}{36}\frac{1}{J^2\hat{c}\hat{g}^{AA}}\right]^{1/2}\left(r^{AB}\frac{\sigma-1}{\sigma}g\cos\phi\right)^{1/2}\left[5\left(\frac{H}{r^{AB}}\right)^{3/2}-\left(\frac{H-Z}{r^{AB}}\right)^{3/2}\right]\frac{1+\hat{c}(\sigma-1)}{\hat{c}(\sigma-1)}\tan\phi, \tag{44}$$

Then, at lowest order in n_B / n_A, Eq. (33) becomes

$$\frac{\partial}{\partial t}\left(\ln\frac{n^B}{n}\right)+u\frac{\partial}{\partial x}\left(\ln\frac{n^B}{n}\right)+\frac{\partial}{\partial x}\left(v_x^B-v_x^A\right)+\frac{\partial}{\partial Z}\left(v_Z^B-v_Z^A\right)=0, \tag{45}$$

Upon introducing $\boldsymbol{F}^B$ and the derivative of π^B in Eq. (40) and keeping only terms at lowest order in n^B/n,

$$v_x^B-v_x^A=-\frac{1}{4}\left(\frac{\pi m^{AB}T}{2m^Am^B}\right)^{1/2}\left[-\frac{3}{2\pi}\frac{1}{g^{AB}}\frac{m^B}{\left(r^{AB}\right)^2nT}\frac{1+\hat{c}(\sigma-1)}{\sigma\hat{c}}g\sin\phi+r^{AB}\frac{\partial}{\partial x}\left(\ln\frac{n^B}{n}\right)\right], \tag{46}$$

and

$$v_Z^B-v_Z^A=-\frac{1}{4}\left(\frac{\pi m^{AB}T}{2m^Am^B}\right)^{1/2}\left[\frac{3}{2\pi}\frac{1}{g^{AB}}\frac{m^B}{\left(r^{AB}\right)^2nT}\left(1-\frac{1}{\sigma}\right)g\cos\phi+2\frac{m^A}{m^{AB}}r^{AB}\frac{\partial\ln T}{\partial Z}+r^{AB}\frac{\partial}{\partial Z}\left(\ln\frac{n^B}{n}\right)\right]. \tag{47}$$

We employ the expression (43) for T in Eqs. (46) and (47), make lengths and velocities dimensionless using r^{AB} and $(gr^{AB})^{1/2}$, respectively, and use the same letters to denote the dimensionless quantities. Then,

$$\begin{aligned}v_x^B-v_x^A=&-\frac{1}{4}\left[\frac{\pi}{2}\frac{m^{AB}}{m^B}\frac{(H-Z)}{\hat{c}\hat{g}^{AA}}\frac{\sigma-1}{\sigma}\cos\phi\right]^{1/2}\\&\times\left[-8\frac{\hat{g}^{AA}}{\hat{g}^{AB}}\frac{m^B}{m^A}\left(\frac{r^A}{r^{AB}}\right)^3\frac{1}{(H-Z)}\frac{1+\hat{c}(\sigma-1)}{\sigma\hat{c}}\tan\phi+\frac{\partial}{\partial x}\left(\ln\frac{n^B}{n}\right)\right]\end{aligned} \tag{48}$$

and

$$\begin{aligned}v_Z^B-v_Z^A=&-\frac{1}{4}\left[\frac{\pi}{2}\frac{m^{AB}}{m^B}\frac{(H-Z)}{\hat{c}\hat{g}^{AA}}\frac{\sigma-1}{\sigma}\cos\phi\right]^{1/2}\\&\times\left[8\frac{\hat{g}^{AA}}{\hat{g}^{AB}}\frac{m^B}{m^A}\left(\frac{r^A}{r^{AB}}\right)^3\frac{1}{(H-Z)}-2\frac{m^A}{m^{AB}}\frac{1}{(H-Z)}+\frac{\partial}{\partial Z}\left(\ln\frac{n^B}{n}\right)\right].\end{aligned} \tag{49}$$

Eqs. (48) and (49) are to be used with

$$\frac{\partial}{\partial t}\left(\ln\frac{n^B}{n^A}\right)+u\frac{\partial}{\partial x}\left(\ln\frac{n^B}{n^A}\right)+\frac{\partial}{\partial x}\left(v_x^B-v_x^A\right)+\frac{\partial}{\partial Z}\left(v_z^B-v_z^A\right)=0, \tag{50}$$

where time has been made dimensionless by $(r^{AB}/g)^{1/2}$ and, when made dimensionless, the mixture velocity of (44) is

$$u=\left(\frac{\pi}{36}\frac{1}{J^2\hat{c}\hat{g}^{AA}}\frac{\sigma-1}{\sigma}\cos\phi\right)^{1/2}\left[5\left(H\right)^{3/2}-\left(H-Z\right)^{3/2}\right]\frac{1+\hat{c}(\sigma-1)}{\hat{c}(\sigma-1)}\tan\phi. \tag{51}$$

These equations describe the time-dependent segregation of dilute species *B* in a steady, uniform, dense flow of species *A* for the simple model of particle interaction derived by Jenkins and Mancini (1987). Simple results for the direction of segregation in an initially uniform mixture (Larcher and Jenkins 2010b) and the steady profile of species concentration (Larcher and Jenkins 2010a) can be obtained directly from the condition that the normal component of the relative velocity vanishes.

The segregation theory just described has not yet been tested in physical experiments or numerical simulations of dense, inclined flows. The theory has the advantage of being based on instantaneous, binary collisions between particles; however, it is not clear that in dense flows the interactions are so simple. Here, we have used the theory for segregation in conjunction with the flow theory of Jenkins and Berzi (2010) that employs phenomenology in an attempt to treat more complicated interactions. There is also a phenomenological theory for size segregation with a structure that is similar but simpler to that describe above that was inspired by physical experiments.

The theory of Thornton, et al. (2006) for size segregation in fluid-saturated, inclined flows attempts to improve upon the mathematical description of kinetic sieving introduced by Lun and Savage (1988). Kinetic sieving involves the downward percolation of small particles through the pore space of a contacting network of large particles that are forced upward. It is based on continuum momentum balances for each particle species that incorporate the rate momentum exchange between the two species, gradients of partial pressures, and gravity. These are the analogs of Eq. (33). Constitutive assumptions for the rate of exchange of momentum and the partial pressures that correspond to Eqs. (44) to (46) result in simple expressions for the diffusion velocities normal to the flow in the absence of diffusive mixing that vanish with the concentration of the other species and with gravity. The incorporation in the momentum exchange of terms proportional to the spatial gradients of species number fractions (Gray and Chugunov 2006) gives the theory the capability to describe diffusive mixing. The resulting theory is simple enough to support elegant analysis of both steady and unsteady segregation, with and without diffusive mixing (e.g., Gray 2010).

Both the kinetic and phenomenological theories have the capability to predict the concentration profiles that exhibit inverse grading - the larger spheres above the smaller - observed in

experiments on dry materials (Lun and Savage 1988, Savage and Valance 2000). The question is whether the particle interactions important to segregation are dominated by near-instantaneous collisions or by longer lasting interactions. If the former, existing methods of phrasing and solving boundary-value problems for size and mass segregation (e.g., Arnarson and Jenkins 2004) can be implemented for these fluid-particle systems.

4. Conclusion

We have reviewed existing laboratory experiments on steady, inclined flows of mixtures of water and a single idealized granular phase that focus on the differences in the depths and the velocity of the two phases; the most recent experimental investigations provide evidence for the importance of collisional exchange of momentum and energy between the particles. Moreover, they show a stratification of rheological regimes within the flow, with some layers dominated by near-instantaneous collisions between grains and others in which particles interact through more sustained contacts. Unfortunately, there is not much data available, particularly for what we have called under-saturated flows. We hope that the present review will stimulate and provide a context for future experimental investigations on debris flows, especially those for which the particle volume flux is greater than the fluid volume flux.

We also have reviewed and extended a two-phase mixture theory that makes use of a relatively simple particle rheology to describe the particle-particle interactions. We have highlighted that the theory is capable of quantitatively reproducing the available laboratory experiments on uniform flows of water and artificial particles. In the context of that theory, the existence of an under-saturated front is sufficient to explain the bulging of a steady granular-fluid wave observed both in laboratory and in the field, without the necessity for change in the particle concentration or size segregation. With respect to the latter, we have outlined a kinetic theory for dense, inclined flows of two types of particles and water as a possible alternative to existing phenomenological theories.

Throughout, we have focused on simple flows of simple particles-fluid systems. While natural debris flows are certainly more complex, our view is that the models that are used to describe them should certainly be capable of describing the simpler situations.

Acknowledgements

The authors are grateful to Professors A. Armanini of Trento University and E. Larcan of the Politecnico di Milano for their support of this collaboration and interest in this work.

References

Armanini, A., Dalrì, C., Fraccarollo, L., Larcher, M., Zorzin, E. (2003) Experimental analysis of the general features of uniform mud-flow. In *Debris-Flow Hazards Mitigation: Mechanics, Prediction, and Assesment* (Rickenmann, D. and Chen, C.-L., Eds.) pp. 423–434, Millpress.

Armanini, A., Capart, H., Fraccarollo, L., Larcher, M. (2005) Rheological stratification in experimental free-surface flows of granular-liquid mixtures. *J. Fluid Mech.* **532** , 269–319.

Armanini, A., Fraccarollo, L., Larcher, M. (2005) Debris Flow. In *Encyclopedia of Hydrological Sciences* (Anderson, M. G., Ed.) Chap. 142, Vol. 4(12), pp. 2173–2186, John Wiley.

Armanini, A., Larcher, M., Fraccarollo, L. (2009) Intermittency of rheological regimes in uniform liquid-granular flows. *Phys. Rev. E* 79, 051306.

Arnarson, B., Jenkins, J.T. (2004) Binary mixtures of inelastic spheres: simplified constitutive theory. *Phys. Fluids* **16**, 4543–4550.

Bagnold, R.A. (1954) Experiments on a gravity-free dispersion of large solid spheres in a Newtonian fluid under shear. *Proc. Roy. Soc. London A* **225**, 49–63.

Balmforth, N.J., Mandre, S. (2004) Dynamics of roll waves. *J. Fluid Mech.* **514**, 1–33.

Berzi, D., Jenkins, J.T. (2008a) A theoretical analysis of free-surface flows of saturated granular-liquid mixtures. *J. Fluid Mech.* **608**, 393–410.

Berzi, D., Jenkins, J.T. (2008b) Approximate Analytical Solutions in a model for highly concentrated granular-liquid Flows. *Phys. Rev. E* **78**, 011304.

Berzi, D., Jenkins, J.T. (2009) Steady, inclined flows of granular-fluid mixtures. *J. Fluid Mech.* **641**, 359–387.

Berzi, D., Jenkins J.T., Larcan E. (2010a) Uniform motion of debris flows over erodible beds. *Proceedings of the First IAHR European Meeting*, Edinburgh, UK (In press).

Berzi, D., Jenkins J.T., Larcan E. (2010b) New formulas for the motion resistance of debris flows. In *Debris Flow 2010*, Milano, Italy (In press).

Brufau, P.G.-N., Garcia-Navarro, P., Ghilardi, P., Natale, L., Savi, F. (2000) 1-D Mathematical modelling of debris flow. *J. Hydraul. Res.* **38**, 435–446.

Capart, H., Young, D. L. (1998) Formation of a jump by the dam-break wave over a granular bed. *J. Fluid Mech.* **372**, 165–187.

Capart, H., Young, D.L., Zech, Y. (2002) Voronoï imaging methods for the measurement of granular flows. *Exp Fluids* **32,** 121–135.

Cassar, C., Nicolas, M., Pouliquen, O. (2005) Submarine granular flows down inclined planes. *Phys. Fluids* **17**, 103301.

Chen, C.L. (1998) Rheological equations in asymptotic regimes of granular flow. *J. Engng Mech.* **124**, 301–310.

Courrech du Pont, S., Gonderet, P., Perrin, B.,Rebaud, M. (2003) Granular avalanches in Fluids. *Phys. Rev. Letts.* **90**, 044301.

Coussot, P. (1994) Steady, laminar flow of concentrated mud suspensions in open channel. *J. Hydraul.Res.* **32**, 535–559.

da Cruz, F., Enman, S., Prochnow, M., Roux, J.-N., Chevoir, F. (2005) Rheophysics of dense granular materials: Discrete simulation of plane shear flows. *Phys. Rev. E* **72**, 021309.

Dallavalle, J. (1943) *Micromeritics.* Pitman.

Davies**,** T.R.H. (1986) Large debris flows: a macro-viscous phenomenon. *Acta Mech.* **63**, 161–178.

Davies, T.R.H. (1988) *Debris Flow Surges -A Laboratory Investigation.* Nr. **96**, Mittellungen der Versuchsanstalt fur Wasserbau, Hydrologie und Glaziologie.

Davies**,** T. R. H. (1990) Debris flow surges - experimental simulation. *New Zealand J. Hyd.* **29**, 18–46.

Drew, D.A., Passman, S.L. (1999) *Theory of multicomponent fluids*. Applied mathematical Sciences 135, Springer.

Fraccarollo, L., Capart, H. (2002) Riemann wave description of erosional dam-break flows. *J. Fluid Mech.* **461**, 183–228.

Fraccarollo, L., Larcher, M., Armanini, A. (2007) Depth-averaged relations for granular-liquid uniform flows over mobile bed in a wide range of slope values. *Gran. Matt.* **9**, 145–157.

Fraccarollo, L., Rosatti, G. (2009) Lateral bed load experiments in a flume with strong initial transversal slope, in sub- and supercritical conditions. *Water Resources Research* **45**, W01419.

Forterre, Y., Pouliquen, O. (2003) Long-surface-wave instability in dense granular flows. *J. Fluid Mech.* **486**, 21–50.

Garzo, V., Dufty, J.W. (1999) Dense fluid transport for inelastic hard spheres. *Phys. Rev. E* **59**, 5895–5911.

Gray, J.M.N.T. (2010) Particle size segregation in granular avalanches: A brief review of recent progress. In *IUTAM-ISIMM Symposium on Mathematical Modeling and Physical Instances of*

Granular Flows (Goddard, J. D., Jenkins, J. T. and Giovine, P., Eds.) pp. 343–362, Vol. 1227, American Institute of Physics.

Gray, J.M.N.T., Chugunov, V.A. (2009) Particle-size segregation and diffusive remixing in shallow granular avalanches. *J. Fluid Mech.* **569**, 365–398.

Herbst, O., Huthmann, M., Zippelius, A. (2000) Dynamics of inelastically colliding spheres with Coulomb friction: Dynamics of the relaxation of translational and rotational energy. *Gran. Matt.* **2**, 211–219.

Hungr, O. (1995) A model for the runout analysis of rapid flow slides, debris flows, and avalanches. *Can. Geotech. J.* **32**, 610–623.

Hungr, O. (2000) Analysis of debris flow surges using the theory of uniformly progressive flow. *Earth Surf. Proc. Lndfrms.* **25**, 483–495.

Iverson, R.M. (1997) The physics of debris flows. *Rev. Geophys.* **35**, 245–296.

Iverson, R.M. (2003) The debris-flow rheology myth. *Debris-Flow Hazards Mitigation: Mechanics, Prediction, and Assesment* (Rickenmann, D. and Chen, C.-L., Eds.) pp. 303–314, Millpress.

Iverson, R.M. (2009) Elements of an improved model of debris-flow motion. In *Powders and Grains 2009* (Luding, S. and Nakagawa, M., Eds.) pp. 1–16, American Institute of Physics.

Jenkins, J.T. (2006) Dense shearing flows of inelastic disks. *Phys. Fluids* **18**, 103307.

Jenkins, J.T. (2007) Dense inclined flows of inelastic spheres. *Gran. Matter* **10**, 47–52.

Jenkins, J.T., Askari, E. (1991) Boundary conditions for granular flows: phase interfaces. *J. Fluid Mech.* **223**, 497–508.

Jenkins, J.T., Askari, E. (1999) Hydraulic theory for a debris flow on a collisional shear layer. *Chaos* **9**, 654–658.

Jenkins, J.T., Berzi, D. (2010) Steady, inclined flow of a mixture of grains and fluid over a rigid base. In *IUTAMM-ISIMM Symposium on Mathematical Modeling and Physical Instances of Granular Flows* (Goddard, J. D., Jenkins, J. T. and Giovine, P., Eds.) pp. 31–40, Vol. 1227, American Institute of Physics.

Jenkins, J.T., Mancini, F. (1987) Balance laws and constitutive relations for plane flows of a dense, binary mixture of smooth, nearly elastic, circular disks. *J. Appl. Mech.* **54**, 28–34.

Jenkins, J.T., Mancini, F. (1989) Kinetic theory for binary mixtures of smooth, nearly elastic spheres. *Phys. Fluids* A **1**, 2050–2057.

Jenkins, J.T., Yoon, D.K. (2002) The influence of different species' granular temperatures on segregation in a binary mixture of dissipative grains. *Phys. Rev. Lett.* **88**, 194301.

Johnson, A.M. (1984) Debris flow. In *Slope Instability* (Brunsden, D. and Prior D.B., Eds.), pp. 257–361, John Wiley.

Jop, P., Forterre, Y., Pouliquen, O. (2005) Crucial role of sidewalls in granular surface flows: consequences for the rheology. *J. Fluid Mech.* **541**, 167–192.

Komatsu, T.S., Inagaki, S., Nakagawa, N., Nasuno, S. (2001) Creep motion in a granular pile exhibiting steady surface flow. *Phys. Rev. Lett.* **86**, 1757–1760.

Kumaran, V. (2009a) Dynamics of dense, sheared granular flows. Part I. Structure and Diffusion. *J. Fluid Mech.* **632**, 109–144.

Kumaran, V. (2009b) Dynamics of dense, sheared granular flows. Part II. The relative velocity distributions. *J. Fluid Mech.* **632**, 145–198.

Larcher, M., Fraccarollo L., Armanini, A., Capart, H. (2007) Set of measurement data from flume experiments on steady, uniform debris flows. *J. Hydraul. Res.* **45,** 59–71.

Larcher, M., Jenkins, J.T. (2009) The influence of size segregation in particle-fluid flows. In *Powders and Grains 2009* (Nakagawa, M. and Luding, S., Eds.), pp. 1055–1058, Vol. 1145, American Institute of Physics.

Larcher, M., Jenkins, J.T. (2010a) Size segregation in dry granular flows of binary mixtures. In *IUTAM-ISIMM Symposium on Mathematical Modeling and Physical Instances of Granular Flows* (Goddard, J. D., Jenkins, J. T. and Giovine, P., Eds.), pp. 363–370, Vol. 1227, American Institute of Physics.

Larcher, M., Jenkins, J.T. (2010b) Particle size and density segregation in dense, dry granular flows. *Proceedings of the First IAHR European Meeting*, Edinburgh, UK, (In press).

McPhee, J. (1989) *The Control of Nature*. Noonday Press.

Midi, G.D.R. (2004) On dense granular flows. *Euro. Phys. J. E* **14**, 341–365.

Mitarai, N., Nakanishi, H. (2005) Bagnold scaling, density plateau, and kinetic theory analysis of dense granular flow. *Phys. Rev. Lett.* **94**, 128001.

Pitman, E.B., Le, L. (2005) A two-fluid model for avalanche and debris flows. *Phil. Trans. R. Soc. A* **363**, 1573–1601.

Pouliquen, O. (1999a) Scaling laws in granular flows down rough inclined planes. *Phys. Fluids* **11**, 542–548.

Pouliquen, O. (1999b) On the shape of granular fronts down rough inclined planes. *Phys. Fluids*, **11,** 1956–1958.

Richardson, J.F., Zaki, W.N. (1954) Sedimentation and fluidization. *Trans. Inst. Chem. Engrs.* **32**, 35–53.

Savage, S.B., Lun, C.K.K. (1988) Particle size segregation in inclined chute flow of dry cohesionless granular solids. *J. Fluid Mech.* 181, 311–335.

Spinewine, B., Capart, H., Larcher, M., Zech, Y. (2003) Three-dimensional Voronoï imaging methods for the measurement of near-wall particulate flows. *Exp Fluids* **34**, 227–241.

Spinewine, B., Capart, H., Fraccarollo, L., Larcher, M. (2010) Laser stripe measurements of near-wall solid fraction in channel flows of liquid-granular mixtures. *Exp Fluids*, Under review.

Takahashi, T. (1978) Mechanical characteristics of debris flow. *J. Hydraul. Div.*, ASCE **104**, 1153–1169.

Takahashi, T. (1980) Debris flow on prismatic open channel. *J. Hydraul. Div.*, ASCE **106**, 381–396.

Takahashi, T. (1981) Debris flow. *Ann. Rev. Fluid Mech.* **13**, 57–77.

Takahashi, T. (1991) *Debris Flow*. Balkema.

Thornton, A.R., Gray, J.M.N.T., Hogg, A.J. (2006) A three-phase mixture theory for particle size segregation in shallow granular free-surface flows. *J. Fluid Mech.* **550**, 1–25.

Tubino, M.A., Lanzoni, S. (1993) Rheology of debris flows: experimental observations and modeling problems. *Excerpta Ital. Contrib. Field Hydraul. Engng.* **7**, 201–236.

Vallance, J.W., Savage, S.B. (2000) Particle segregation in granular flows down chutes. In *IUTAM Symposium on segregation in granular materials* (Rosato, A. D. and Blackmore, D. L., Eds.) pp. 31–51, Kluwer.

Zenit, R., Hunt, M.L. (1998) The impulsive motion of a liquid resulting from a particle collision. *J. Fluid Mech.* **375**, 345–361.